

3 WATER QUALITY

DSM2-QUAL is a water quality model based on the Branched Lagrangian Transport Model, a public domain code written by Harvey E. Jobson and his colleagues at the U.S. Geological Survey. The main advantages of DSM2-QUAL over the Department's existing water quality module include:

- DSM2-QUAL can simulate the transport of multiple constituents in the Delta. Internal kinetic reactions can be incorporated, and the decay or growth of each constituent can be numerically accounted for.
- DSM2-QUAL does not need to know the shape of the cross-section. The model needs the flow, flow area, and top width. All the other parameters are recalculated.

Bodies of water are divided into parcels. The movements of these parcels within the channels are controlled using the flow data provided in the tide file. The size of these parcels usually do not change as long as they are entirely within one channel, but once they reach a junction, incoming parcels are merged and/or split to form new parcels. The model continues to update the concentration of each of the simulated constituents during each time step. Dispersion only takes place at the interface between the parcels. However, full mixing at the junctions is assumed.

The following describes the Delta Modeling Section's efforts to improve and add new features to DSM2-QUAL during the past year. The development of subroutines to model nonconservative constituents and a preliminary model evaluation are also described.

Hydro File

The original version of BLTM reads hydrodynamic information, provided at every time step, from an ASCII file. This had several disadvantages, as briefly described in Chapter 2. The main disadvantage is that the file can be massive for a long-term model run. The other disadvantage is that the user is forced to use a time step that matched the hydro file. To change the size of the time step, the user must develop a new hydro file with the matching time step. In DSM2-QUAL, the user is now free to choose the size of the time step, and all the values are properly averaged.

Open Water Reservoir

An open water reservoir is currently modeled as a tank of water. The concentration of each of the constituents is assumed to be constant throughout the reservoir and is updated every time step. The following describes how the concentration of a conservative constituent is calculated based on different cases. To illustrate this, a reservoir is considered with two connecting junctions. Three different cases can be encountered depending on the direction of the two flow components. Updated concentrations are denoted with primes:

Case 1: Flow Entering the Reservoir from Both Junctions

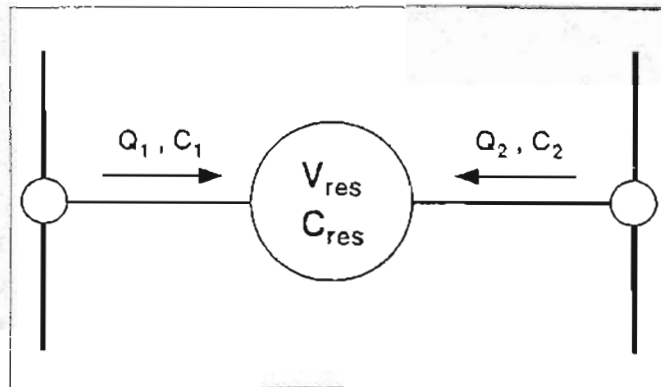


Figure 3-1. Channel Schematics for Case 1

$$V'_{res} = V_{res} + (Q_1 + Q_2) * \Delta t \quad (3-1)$$

$$C'_{res} = \frac{V_{res} * C_{res} + Q_1 * C_1 * \Delta t + Q_2 * C_2 * \Delta t}{V'_{res}} \quad (3-2)$$

where

V_{res} = Water volume in the reservoir

C_{res} = Constituent concentration in the reservoir

Q_1, Q_2 = Flow rate entering the reservoir

C_1, C_2 = Constituent concentration assigned to Q_1 and Q_2

Δt = time step

Case 2: Flow Entering the Reservoir from One Junction and Leaving from the Other

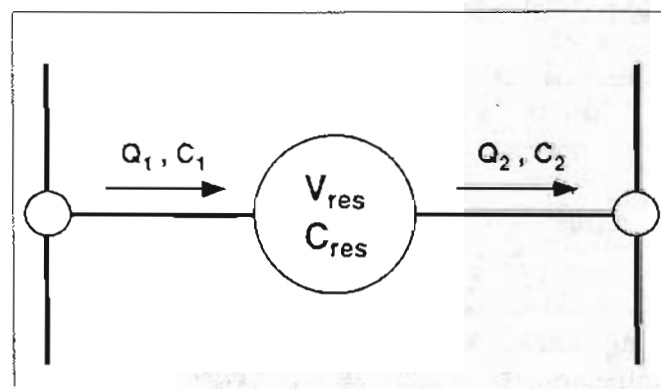


Figure 3-2. Channel Schematics for Case 2

$$C_2' = C_{res} \quad (3-3)$$

$$V_{res}' = V_{res} + (Q_1 - Q_2) * \Delta t \quad (3-4)$$

$$C_{res}' = \frac{V_{res} * C_{res} - Q_2 * C_{res} * \Delta t + Q_1 * C_1 * \Delta t}{V_{res}'} \quad (3-5)$$

Case 3: Flow Leaving the Reservoir from Both Junctions

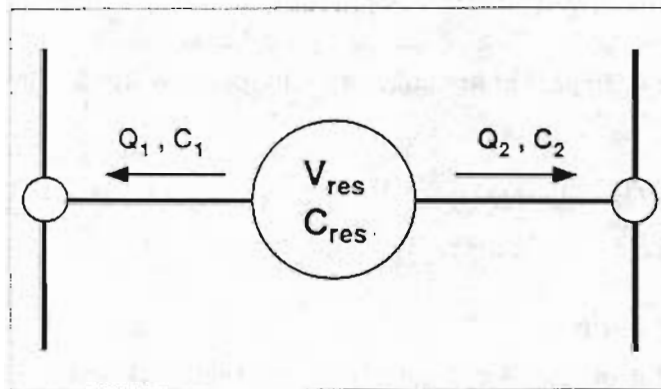


Figure 3-3. Channel Schematics for Case 3

$$C_1' = C_{res} \quad (3-6)$$

$$C_2' = C_{res} \quad (3-7)$$

$$V_{res}' = V_{res} - (Q_1 + Q_2) * \Delta t \quad (3-8)$$

$$C_{res}' = C_{res} \quad (3-9)$$

If the constituent is nonconservative, the growth or decay of the constituent is first determined, and a new C_{res} is computed. From there, the procedure for the conservative constituent is followed.

Agricultural Diversions and Returns

The original version of BLTM has the option of assigning flows (either inward or outward) to any grid point within a channel. However, flow estimates for agricultural drainage (Q_{ag}) and diversions (Q_{ch}) are currently provided to DSM2 at specified junctions by the Delta Island Consumptive Use (DICU) model. Thus DSM2-QUAL was modified to include this possibility. Future model enhancements will relax this constraint. The following example illustrates the impact of agricultural diversions and returns (see Figure 3-4).

$$C_3 = C_{ch} = \frac{Q_1 * C_1 + Q_2 * C_2 + Q_{ag} * C_{ag}}{Q_1 + Q_2 + Q_{ag}} \quad (3-10)$$

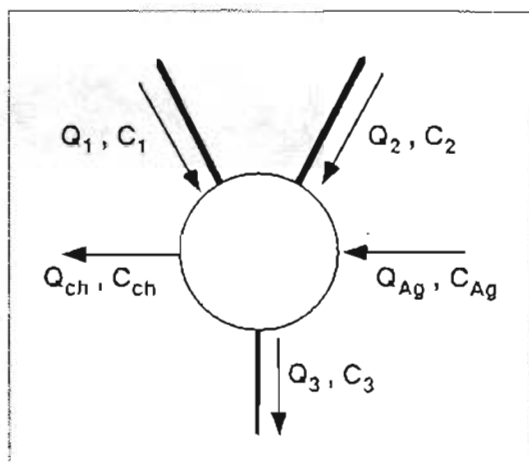


Figure 3-4. Impact of Agricultural Drainage on Water Quality

$$Q_3 = Q_1 + Q_2 + Q_{ag} - Q_{ch} \quad (3-11)$$

Equation 3-11 is enforced in DSM2-HYDRO.

Mass Tracking Routine

MTR is a very powerful and useful tool that lets the user keep track and account for all simulated water quality constituents. First, the amount (or mass, M) of each of the constituents in the Delta is calculated:

$$M = M_{res} + M_{chan} \quad (3-12)$$

where

M_{res} = The initial constituent mass in the reservoirs at the beginning of the time step

M_{chan} = The initial constituent mass in the channels at the beginning of the time step

Then the mass of each of the constituents injected by all the incoming flows in one time step is calculated. This calculation includes all the rim flows, agricultural returns, and the flood tide:

$$M_{in} = M_{rim} + M_{ag} + M_{flood} \quad (3-13)$$

where

M_{in} = The constituent mass injected by incoming flows

M_{rim} = The constituent mass injected by rim flows

M_{ag} = The constituent mass injected by agricultural returns

M_{flood} = The constituent mass injected by the flood tide

Next, the mass of each of the constituents released by outgoing flows in one time step is calculated. This calculation includes all the exports, channel diversions, and the ebb tide:

$$M_{out} = M_{export} + M_{ch} + M_{ebb} \quad (3-14)$$

where

M_{out} = The constituent mass removed by outgoing flows

M_{export} = The constituent mass removed by exports

M_{ch} = The constituent mass removed by channel diversions

M_{ebb} = The constituent mass removed by the ebb tide

In addition to the physical transport of the constituents, there can be kinetic reactions among the nonconservative constituents, resulting in internal growth or decay. For each of the nonconservative constituents, the amount of growth (M_{growth}) or decay (M_{decay}) is calculated for the entire Delta.

The amount of constituents at the end of the time-step can then be determined using the above components:

$$M' = M + M_{In} - M_{out} + M_{growth} - M_{decay} \quad (3-15)$$

The above value can be compared against the calculated amount of constituents left in the Delta. See Equation 3-12.

$$M' = M'_{res} + M'_{chan} \quad (3-16)$$

The results of Equation (3-15) should be exactly equal to Equation (3-16). If all the calculations above are done correctly, and the results differ, the reason can be attributed to one of two factors.

- **Incorrect formulation.** Mass is being lost or gained without being properly accounted for—an indication that there is probably a flaw (which needs to be fixed) in the program.
- **Round off error.** Tens of thousands of calculations are needed to obtain the results of equations (3-15) and (3-16). Some of the parameters in the above equations are the results of DSM2-HYDRO simulations, which in turn require hundreds of thousands of calculations. Computers can store numbers with a limited precision. The loss of precision may be insignificant for a given number but may in fact become significant after numerous accumulations.

One use of the MTR is to check for the problems just described. Many problems have been detected and corrected using this routine. MTR aided in the development of the reservoir routine and accounting for agricultural drainages and channel diversions. Due to the very complex network representing the Delta and other complicated problems such as flow reversals, it would be very easy to overlook all the possible scenarios and events.

MTR detected a flaw in the original BLTM formulation. The problem was in a part of the code where it was combining two small parcels of water into one. Under certain conditions, the smallest parcel in a channel simply disappeared. Without the aid of MTR, it would have been almost impossible to detect this problem.

The most important application of MTR is probably its use as an investigative tool. In a hypothetical study, a dye can be injected in a certain location, and MTR can monitor how the dye is spreading. For every time step, MTR reports (in terms of percentages) the amount of the dye in the Delta channels and reservoirs, the amount which has left the Delta from each outlet location, and, in case of nonconservative constituents, the amount of growth or decay. This information can help evaluate the impact of various sources on the

water quality at a particular location. MTR is also robust enough so that it can be easily modified to focus on a particular location and extract all the desired information. In essence, MTR can function like a particle tracking model, but it works on a homogeneous solution rather than individual particles.

Round-Off Error on Continuity at a Junction

As mentioned before, hydrodynamic information is averaged over a specified time interval inside DSM2-HYDRO. This model enforces continuity at every junction, that is, the sum of the flows entering the junction must equal the sum of the flows leaving the junction. Due to the extra calculations performed during the averaging and the limited precision, there can be small imbalances, thus artificially creating or removing mass from the system. The amount of this imbalance may seem infinitesimally small; however, it can add up to a significant amount when accumulated over all the junctions and over time. The amount of this error can potentially grow larger with larger time intervals used in the tide file. This problem was detected using MTR.

The following describes a possible remedy, which is currently implemented in DSM-QUAL. Figure 3-5 illustrates a junction with three connecting channels. The flows Q_1 , Q_2 , and Q_3 are read from the hydro file.

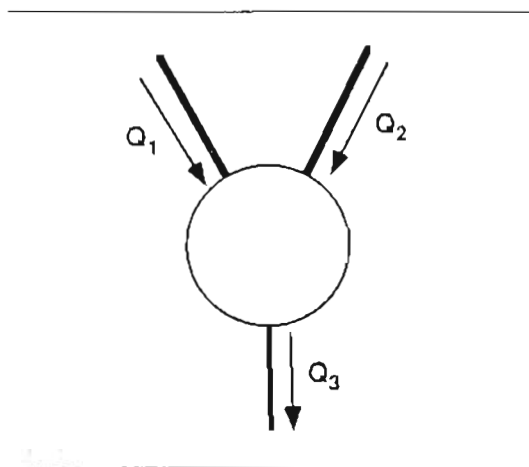


Figure 3-5. Schematics of a Typical Junction Before Flow Corrections

Continuity requires that:

$$Q_1 + Q_2 - Q_3 = 0 \quad (3-17)$$

However, due to possible round off error, in general there is a small imbalance (E). The idea is to distribute this imbalance to the connecting channels. One idea is simply to divide this error equally among the three channels. However, this simple division is not recommended since a nonzero flow can result in a channel with a barrier. A superior approach is to divide this imbalance in proportion to the absolute magnitude of the flows in the three channels:

$$E = Q_1 + Q_2 - Q_3 \quad (3-18)$$

$$\Sigma Q = |Q_1| + |Q_2| + |Q_3| \quad (3-19)$$

$$Q_1^c = Q_1 - \frac{E * |Q_1|}{\Sigma Q} \quad (3-20)$$

$$Q_2^c = Q_2 - \frac{E * |Q_2|}{\Sigma Q} \quad (3-21)$$

$$Q_3^c = Q_3 - \frac{E * |Q_3|}{\Sigma Q} \quad (3-22)$$

where the superscript C indicates the corrected values

The following example illustrates the application of the correction technique described above, assuming $Q_1=1000$. cfs, $Q_2=2000$. cfs, and $Q_3=2999.99994$ cfs.

Error in continuity from Equation 3-18:

$$E = 1000. + 2000. - 2999.99994 = 0.00006 \text{ cfs}$$

Sum of all the flows from Equation 3-19:

$$\Sigma Q = 1000. + 2000. + 2999.99994 = 5999.99994 \text{ cfs}$$

Thus the corrected values are:

$$Q_1^c = 1000. - 0.00006 * 1000./5999.99994 = 999.99999 \text{ cfs}$$

$$Q_2^c = 2000. - 0.00006 * 2000./5999.99994 = 1999.99998 \text{ cfs}$$

$$Q_3^c = 2999.99994 + 0.00006 * 3000./5999.99994 = 2999.99997 \text{ cfs}$$

After correction:

$$Q_1^c + Q_2^c - Q_3^c = 0$$

Therefore, continuity is exactly satisfied. It can be shown that in case of a barrier, the magnitude of the correction would also be zero, thus maintaining the status of the barrier.

Nonconservative Kinetics

New subroutines for modeling nonconservative constituents in the Delta have been completed. These routines are structured in modular form so that they are easy to understand and can be extended to simulate additional constituents with minimum change in existing routines, if such needs arise in the future. Flexibility has been built into the model so that any combination (one, a few, or all) of the variables can be modeled as suited to the needs of the user. The model, in its present form, can simulate the following variables:

1. Temperature
2. Biochemical oxygen demand (BOD)
3. Dissolved oxygen
4. Organic nitrogen
5. Ammonia nitrogen
6. Nitrite nitrogen
7. Nitrate nitrogen
8. Organic phosphorus
9. Dissolved (inorganic) phosphorus
10. Algae (phytoplankton)
11. Arbitrary conservative or nonconservative constituent.

Refer to the Fifteenth Annual Progress Report, 1994, for a description of the mathematical relationships that describe the constituent reactions and interactions. The interactions among water quality constituents are shown in Figure 3-6. A few important relationships that were not detailed in the 1994 report are described below. Subroutines are described briefly later in this section.

Dissolved Oxygen Saturated Concentration

The solubility of dissolved oxygen in water decreases with increasing temperature and salinity. Among about half a dozen or so expressions for DO saturation concentration as a function of temperature reported in the literature, the following algorithm recommended by American Public Health Association (1985) and rated the best by Bowie et al. (1985), was coded in the model:

$$\ln O_{sf} = -139.34411 + \frac{1.575701 \cdot 10^5}{T} - \frac{6.642308 \cdot 10^7}{T^2} + \frac{1.24380 \cdot 10^{10}}{T^3} - \frac{8.621949 \cdot 10^{11}}{T^4} \quad (3-23)$$

where O_{sf} is the "freshwater" DO saturation concentration in mg/L at 1 atm and T is temperature in $^{\circ}\text{K}$. The effect of salinity on DO saturation is incorporated as shown below (APHA 1985):

$$\ln O_{ss} = \ln O_{sf} - S^* \left[0.7674 \cdot 10^{-2} - \frac{1.0754 \cdot 10}{T} + \frac{2.1407 \cdot 10^3}{T^2} \right] \quad (3-24)$$

where O_{ss} is the "saline water" DO saturation concentration in mg/L at 1 atm and S is salinity in ppt. The effect of barometric pressure on DO saturation is to increase the saturation value and is expressed as:

$$O_s = O_{ss} P \left[\frac{1 - (P_{wv}/P)(1 - \phi P)}{(1 - P_{wv})(1 - \phi)} \right] \quad (3-25)$$

where O_s is the DO saturation at pressure P in mg/L, P is the nonstandard pressure in atm, P_{wv} is the partial pressure of water vapor in atm calculated from:

$$\ln P_{wv} = 11.8571 - \frac{3840.70}{T} - \frac{216961}{T^2} \quad (3-25a)$$

$$\phi = 0.000975 - 1.426 \times 10^{-5} t + 6.436 \times 10^{-8} t^2 \quad (3-25b)$$

$$t = \text{temperature in } ^\circ\text{C} = T - 273.150 \quad (3-25c)$$

Atmospheric Reaeration

Reaeration, a process by which oxygen is exchanged between the atmosphere and a water body, is one of the main sources of oxygen in aquatic systems. The transfer rate of oxygen from air to water may be represented by:

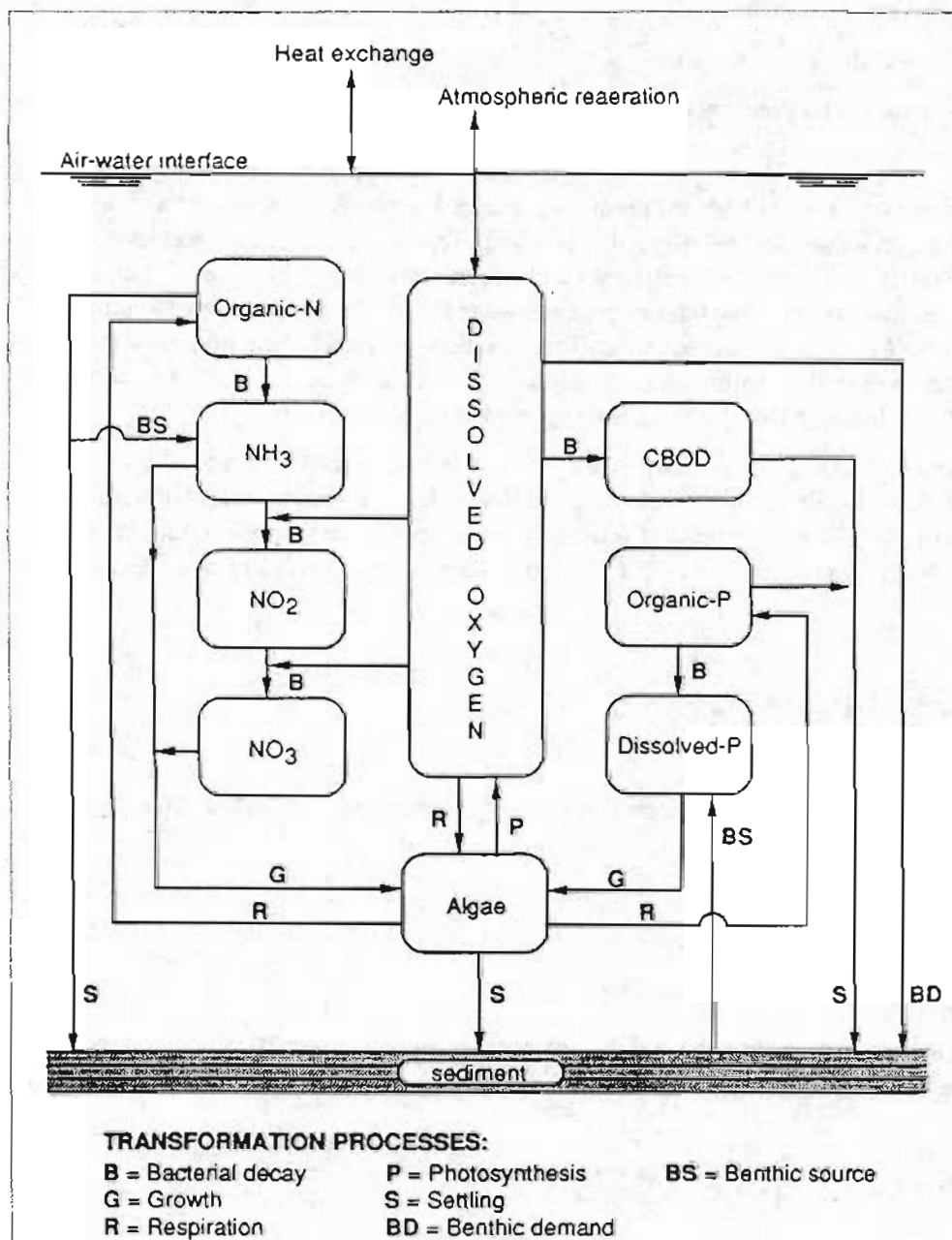


Figure 3-6. Interaction Among Water Quality Constituents in the Model

$$\frac{d[O]}{dt} = k_2 (O_s - O) \quad (3-26)$$

where O_s and O are the oxygen concentrations at saturation and oxygen concentrations of the water body, respectively, and k_2 is the reaeration coefficient. The oxygen transfer coefficient in natural waters depends on (Thomann and Mueller, 1987 and Gromiec, 1989):

- temperature
- internal mixing and turbulence
- mixing due to wind
- waterfalls, dams, rapids
- surface active reagents

Numerous equations are available for predicting reaeration coefficients, giving a wide range of predicted values for specific hydraulic conditions (Rathbun, 1977). Reviews of predictive models for reaeration coefficient can be found in Bowie et al. (1985), Rathbun (1977) and Gromiec (1989). For tidal rivers and estuaries, one of the most widely applied models is the O'Connor-Dobbins equation. This equation, adapted for the present water quality model, is described below. A more detailed discussion of alternative reaeration rate formulations, including a list of references, is provided by Rajbhandari (1995)

O'Conner and Dobbins' (1956) equations were based on their analysis of reaeration mechanisms that considered the rate of surface renewal through internal turbulence. They recommended the following equation for the reaeration coefficient for moderately deep to deep channels (approximately between 1 ft to 30 ft. deep) and velocities between 0.5 ft/s and 1.6 ft/s:

$$k_2 (20^\circ\text{C}) = (D_m \bar{u})^{0.5} d^{-1.5} \quad (3-27)$$

where D_m is the molecular diffusion coefficient, L^2/T . The above equation is often expressed as:

$$k_2 (20^\circ\text{C}) = 12.9 \bar{u}^{0.5} d^{-1.5} \quad (3-28)$$

where \bar{u} is the mean velocity (ft/s) and d is the average stream depth (ft). The effect of temperature on the reaeration coefficient is represented by:

$$k_2 (t^\circ\text{C}) = k_2 (20^\circ\text{C}) (\Theta)^{(t - 20)} \quad (3-29)$$

The numerical value of Θ depends on the mixing conditions of the water body. Reported values range from 1.008 to 1.047 (Bowie et al, 1985). In practice a value of 1.024 is often used (Thomann and Mueller, 1987, Gromiec, 1989 etc.) which has been adopted for the model.

Subroutines

Figure 3-7 is presented to highlight the main processes involved in the dynamic simulation of water quality in the Delta. A brief description of the newly developed subroutines is provided below. Figures are included for a few routines to illustrate the main processes.

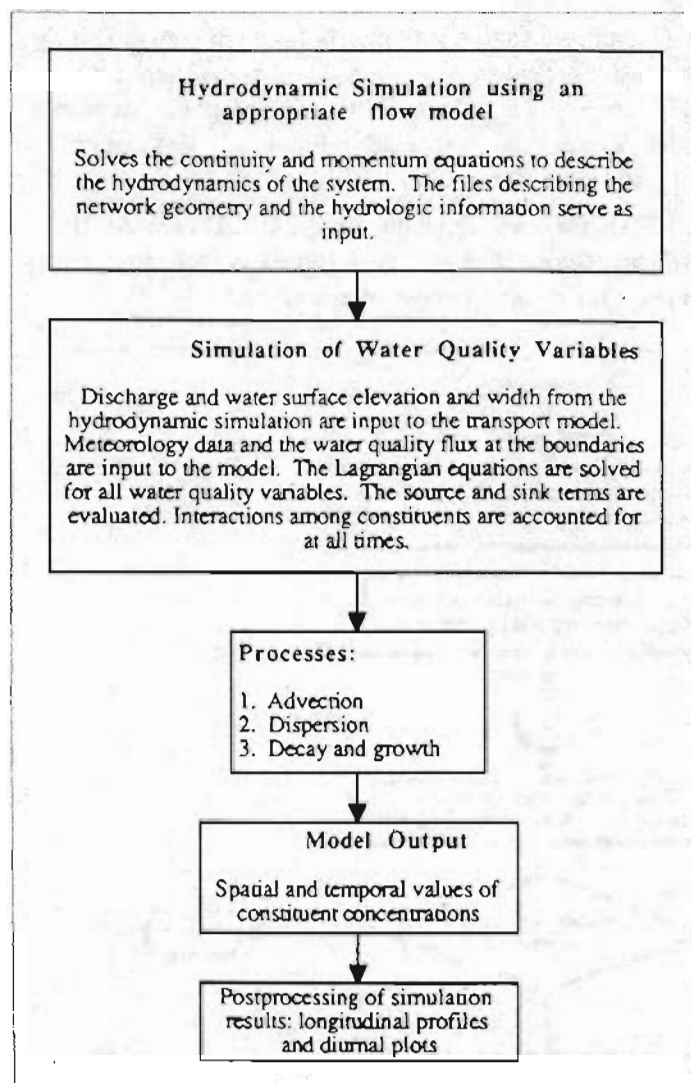


Figure 3-7. Flow Chart for the Dynamic Simulation of Water Quality Variables in the Delta

KINETICS

The main function of this subroutine is to update constituent concentrations at each time step. It is called by BLTM's parcel tracking subroutine (ROUTE) for every parcel at each time step. The flowchart (Figure 3-8) shows the logic of the subroutine. It has also been extended to simulate kinetics in 'reservoirs' in the Delta.

CALSCSK

This subroutine builds a source/sink matrix for each constituent by calling each constituent subroutine. Individual constituent routines are listed in Figure 3-9. Flowcharts for three principal constituents (DO, algae, temperature) are presented in Figures 3-10 through 3-12 for illustrative purposes.

HEAT

Subroutine HEAT has been adapted from the USEPA QUAL2E model (Brown and Barnwell, 1987) with some restructuring. This version computes the net short wave solar radiation

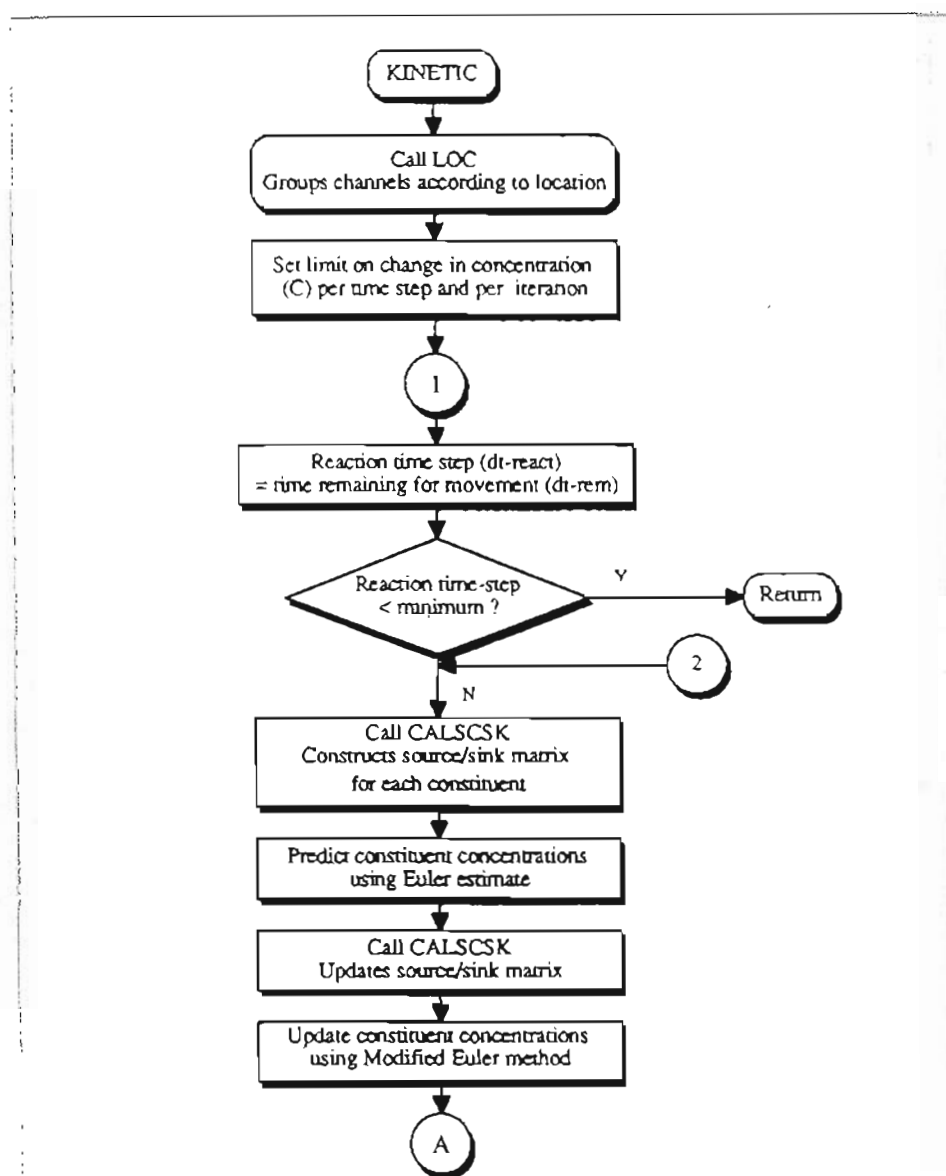


Figure 3-8. Flow Chart for Subroutine KINETIC

and the long wave atmospheric radiation once every hour (Figure 3-13).

MET

A call statement to this subroutine (for every hour) was added to the main BLTM routine. Meteorology data read by this subroutine are used in computation of heat components as shown in Figure 3-13.

RATE

Physical, chemical and biological rate coefficients are read in this subroutine. Some of these coefficients are constant throughout the system; some vary by location; and some are temperature-dependent. A list of these coefficients, including their ranges, is provided in Table 3-1 (Brown and Barnwell, 1987). Temperature coefficients used in the model are listed in Table 3-2.

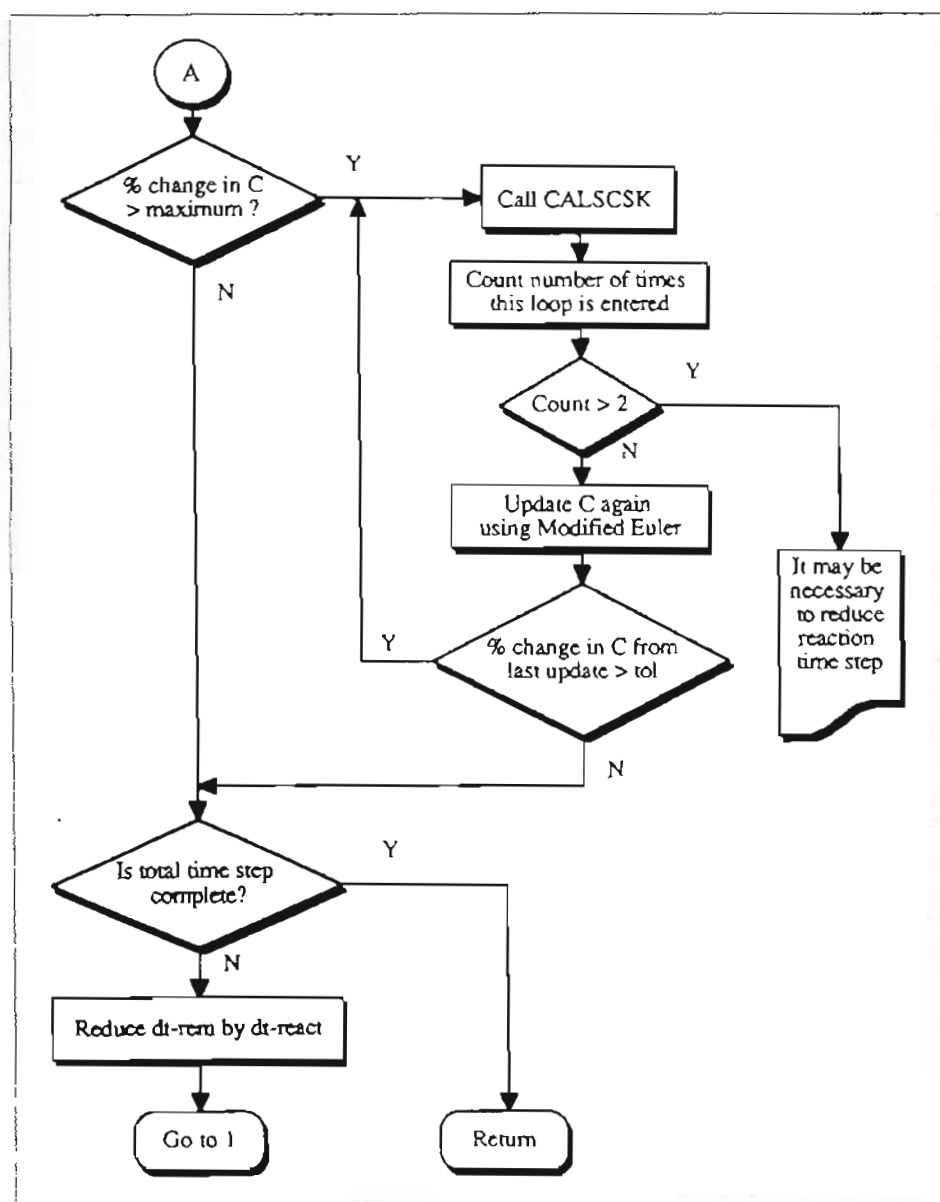


Figure 3-8 (continued)

LOC

This subroutine groups channels by their number or location. The grouping allows the input of spatially varying rate coefficients in the model.

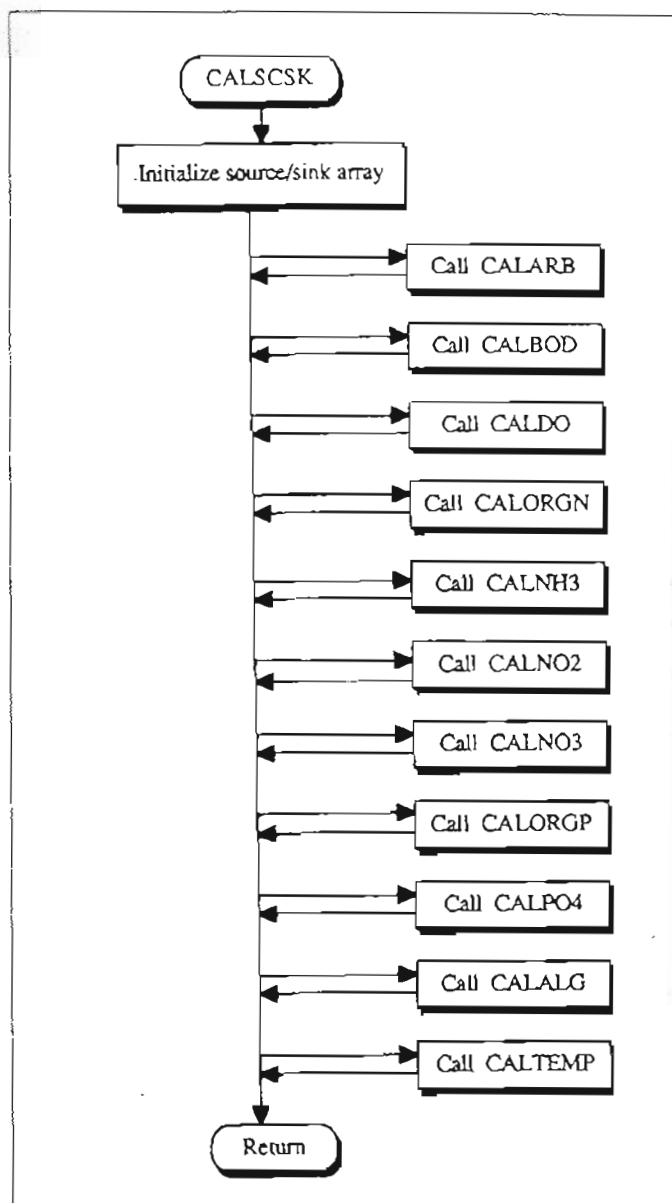


Figure 3-9. Flow Chart for Subroutine
CALSCSK

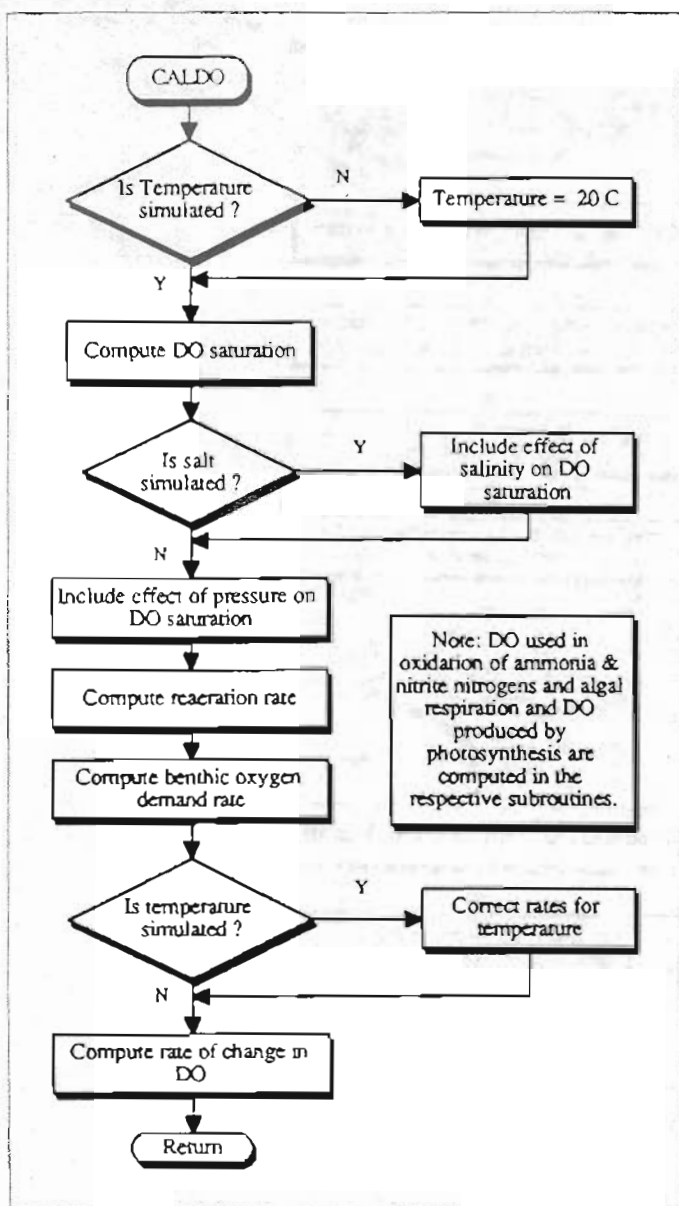


Figure 3-10. Flow Chart for Subroutine CALDO

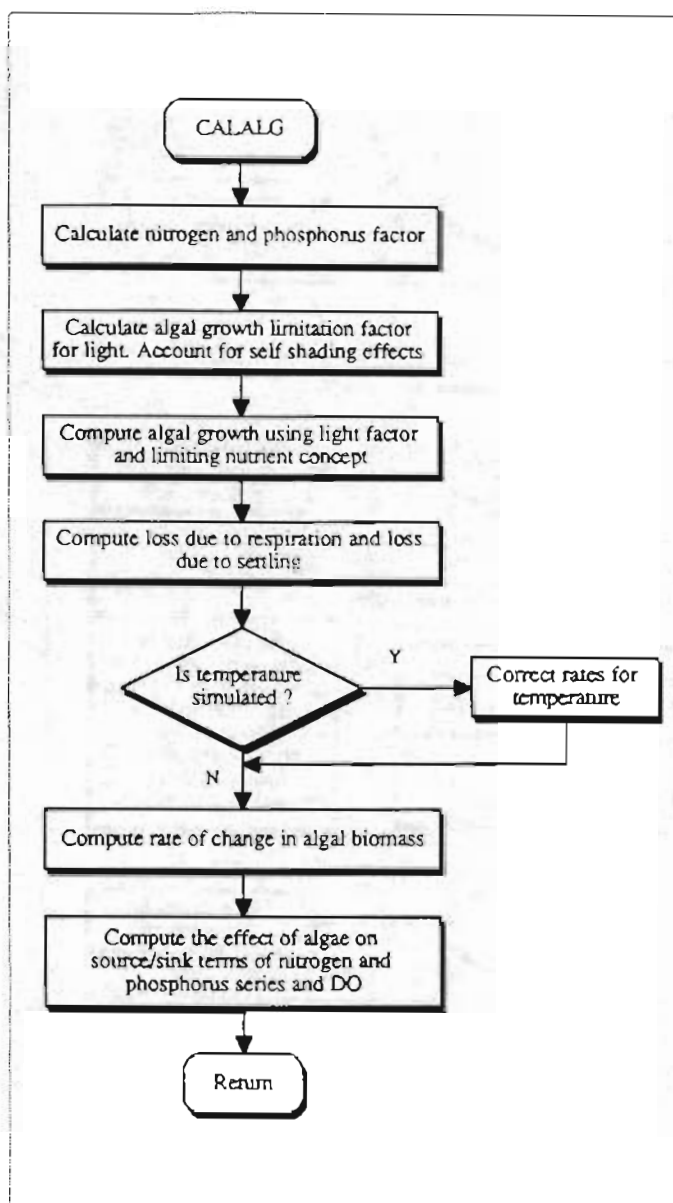


Figure 3-11. Flow Chart for Subroutine CALALG (algae)

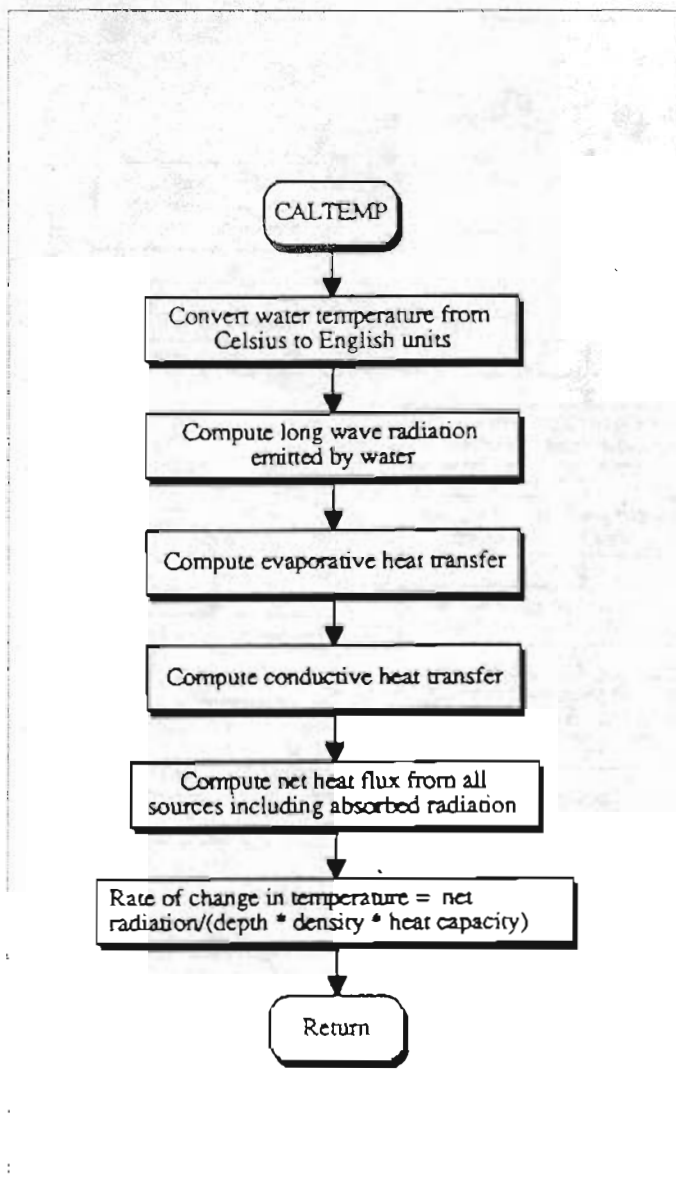


Figure 3-12. Flow Chart for Subroutine CALTEMP

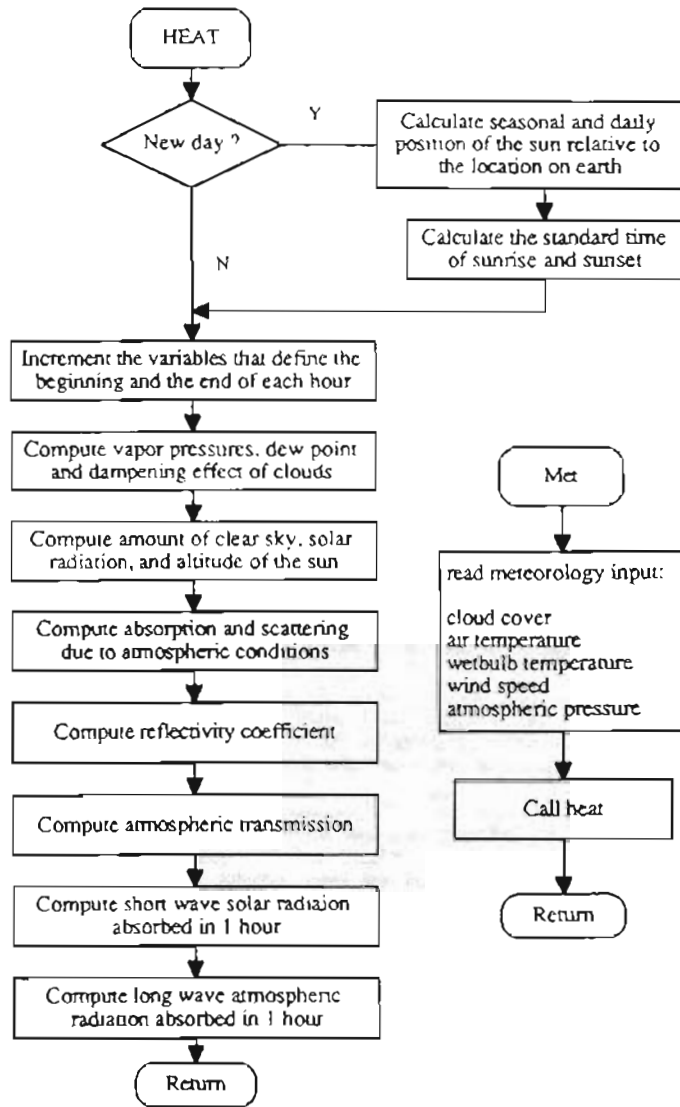


Figure 3-13. Flow Chart for Subroutine HEAT

Table 3-1. Typical Ranges for Reaction Coefficients

Global coefficient values. Variable names shown are the same as used in the FORTRAN code.

alph(5)	oxygen used in conversion of ammonia to nitrite	3.0 - 4.0
alph(6)	oxygen used in conversion of nitrite to nitrate	1.0 - 1.14
prefn	algal preference factor for ammonia	0 - 1.0
alph(7)	chlorophyll-a to biomass ratio	10 - 100
alph(1)	fraction of algal biomass which is nitrogen	0.07 - 0.09
alph(2)	fraction of algal biomass which is phosphorus	0.01 - 0.02
alph(3)	oxygen produced in photosynthesis	1.4 - 4.8
alph(4)	oxygen consumed with respiration	1.6 - 2.3
klght_half	half saturation constant for light	0.02 - 0.10
knit_half	half saturation constant for nitrogen	0.01 - 0.30
kpho_half	half saturation constant for phosphorus	0.001 - 0.05
xlam0	non-algal light extinction coefficient	variable
xlam1	linear algal self shading coefficient	0.002 - 0.02
xlam2	nonlinear algal self shading coefficient	0.0165

Location dependent coefficient values. Variable names shown below are the same as used in the text of the 1994 Annual Report. These coefficients are described by the array *rcoef* in the FORTRAN code.

k1	BOD decay rate	0.02 - 3.4
k3	BOD settling rate	-0.36 - 0.36
k4	benthic source rate for DO	variable
karb	decay rate for arbitrary non-cons. constituent	variable
s6	settling rate for arbitrary non-cons. constituent	variable
s7	benthic source rate for arbitrary non-cons. constituent	variable
mumax	maximum algal growth rate	1.0 - 3.0
resp	algal respiration rate	0.05 - 0.5
s1	algal settling rate	0.5 - 6.0
kn-org	organic nitrogen decay rate	0.02 - 0.4
s4	organic nitrogen settling rate	0.001 - 0.1
kn	ammonia decay rate	0.1 - 1.0
s3	benthic source rate for ammonia	variable
kni	nitrite decay rate	0.2 - 2.0
kp-org	organic phosphorus decay rate	0.01 - 0.7
s5	organic phosphorus settling rate	0.001 - 0.1
s2	benthic source rate for dissolved P	variable

Note: rates are in units per day except when specified.

Table 3-2. Temperature Coefficients for Reaction Rates

Constituent	Reaction type	Temperature coefficient	Variable (FORTRAN)
BOD	decay	1.047	thet(1)
	settling	1.024	thet(2)
DO	reaeration	1.024	thet(3)
	benthic demand	1.060	thet(4)
ORGANIC-N	decay	1.047	thet(5)
	settling	1.024	thet(6)
AMMONIA-N	decay	1.083	thet(7)
	benthic source	1.074	thet(8)
NITRITE-N	decay	1.047	thet(9)
ORGANIC-P	decay	1.047	thet(10)
	settling	1.024	thet(11)
DISSOLVED-P	benthic source	1.074	thet(12)
ALGAE	growth	1.047	thet(13)
	respiration	1.047	thet(14)
	settling	1.024	thet(15)

Preliminary Model Evaluation

A preliminary evaluation of the extended BLTM model was conducted by applying the model to the Delta. This section describes the earlier stages of calibration and verification (site-specific) in the region including the Stockton Ship Channel. Figure 3-14 shows water quality monitoring stations in the San Joaquin River in the vicinity of Stockton, both upstream and downstream of the city's waste water discharge.

The survey periods September 20, 1988 and October 12, 1988 were chosen for model calibration and verification because of the unique hydrodynamic conditions prevailing in these periods and availability of water quality data. The unique hydrodynamic conditions were due in part to placement of a rock barrier at the head of Old River during the period September 22-28. The barrier causes more water to flow downstream in the San Joaquin River toward Stockton and less into Old River toward Clifton Court. Modeling of the two

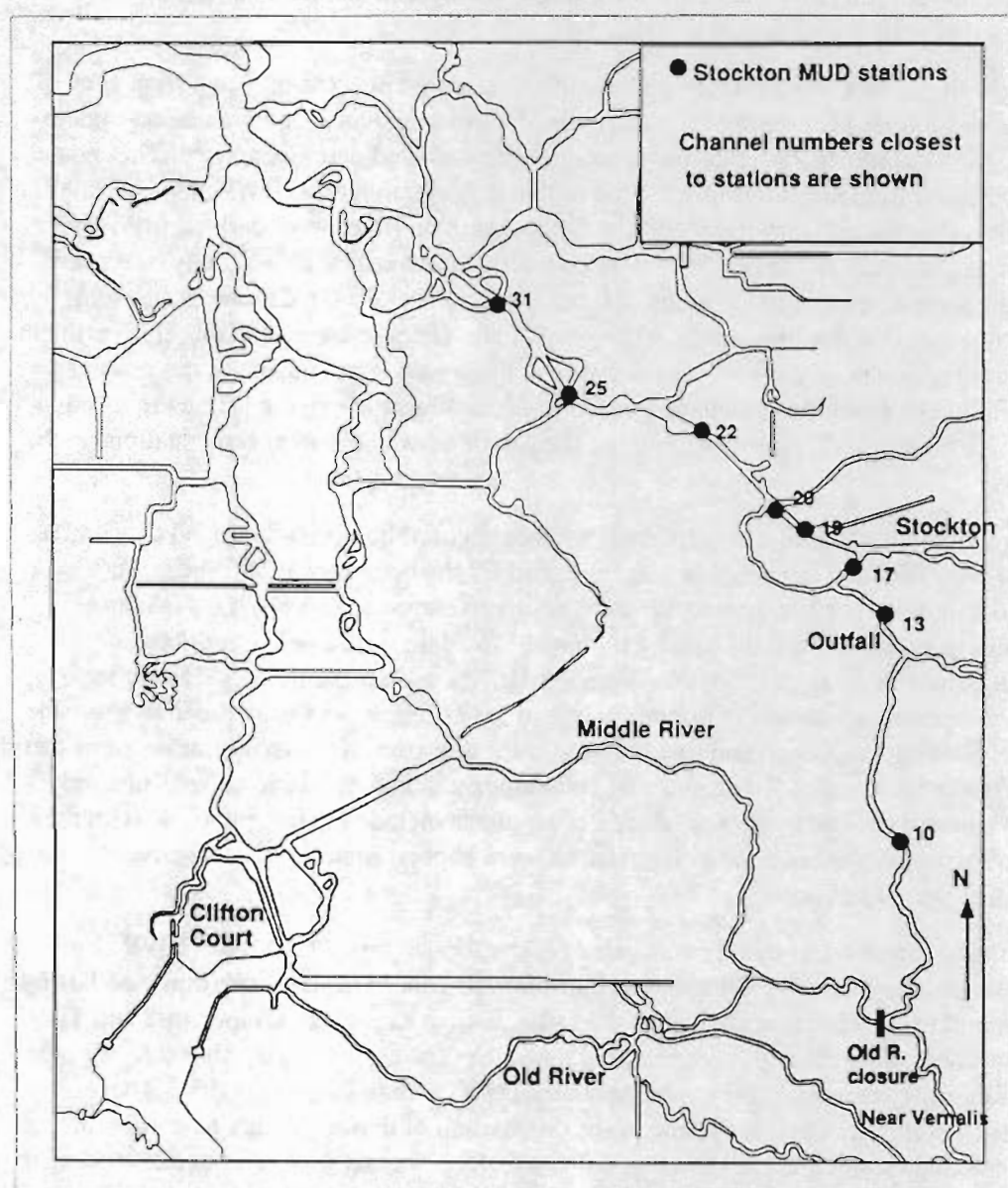


Figure 3-14. Monitoring Stations in San Joaquin River Near Stockton

scenarios provides interesting alternatives of local hydrology and hydraulic behavior as well as changes based on daily flow configurations and water quality.

Model Input

Hydrology. Average daily flows reported in DWR Dayflow Data Summary for 1988 were used for the San Joaquin, Sacramento and Mokelumne River inflows and the State Water Project (SWP), Central Valley Project (CVP) and the Contra Costa Water District (CCWD) withdrawals. Effluent flows from the City of Stockton waste water treatment plant were obtained from the monthly laboratory data file of the Stockton Municipal Utilities District (Huber, pers. comm., 1995). Clifton Court intake gate (opening and closing) schedules were obtained from the monthly operation report (DWR, 1988). Agricultural withdrawals and return flows, which are also input to the model, were based on the Department of Water Resources' monthly estimates. Hydrologic and hydrodynamic data for both simulation periods are presented in Table 3-3.

Water Quality. Since water quality grab sample data were collected only at a frequency of one or two samples per month near model boundaries in the San Joaquin and Sacramento Rivers, and at Martinez, observations closest to the simulated dates were used. These data were extracted from the Water Quality Surveillance Program report (DWR, 1990). Data for Freeport on the Sacramento River and for the Mokelumne River were derived from Water Resources Data (USGS, 1989, 1990). Stockton effluent data, available at daily or weekly intervals, were also input to the model (Huber, pers. comm., 1995). Chlorophyll-a and orthophosphate data for the months of September and October were available from effluent monitoring on a monthly basis only for 1989; so these values were used for the present simulations. All input data, including some at selected locations in the Delta, are listed in Tables 3-3 through 3-7. Figure 3-15 shows the locations of these monitoring stations in the Delta.

To allow representation of diurnal values, whenever possible, hourly averaged concentrations of DO, TDS and temperature were assigned for the boundary at Martinez. Since such detailed data were not available at Vernalis, hourly averaged values of DO, TDS, and temperature available from the nearby station at Mossdale were used as approximate representations of these quantities for Vernalis. Hourly averaged data provided for the simulation period are shown in Figures 3-16 and 3-17. Figure 3-18 is included to show the trend of field data at Rough and Ready Island, near Stockton. No such approximations could be made for the Sacramento River, since no continuously monitored stations were situated near this boundary. Qualities of all eleven constituents included in the model, as with the eight constituents applied at other boundaries, were kept constant for the effective simulation period (25 hours).

Agricultural return water quality was based on an estimate using 1964 data (DWR, 1967). Flow weighted averages of nitrogen and phosphorous concentrations were computed using data from thirteen sampling stations in the Delta. Estimates for DO, temperature and TDS concentrations were obtained by averaging the values corresponding to three sub-regions in the Delta for the particular months simulated (MWQI Data Request, 1995). These subregions were classified according to the distribution of dissolved organic carbon in the Delta. Since data on chlorophyll-a was not available, it was set to a value corresponding to an average for the Sacramento and San Joaquin rivers during the period of simulation.

Hourly meteorological conditions for September 20 and October 18 of 1988 were generated from climatological data at Sacramento Executive Airport (NOAA, 1988).

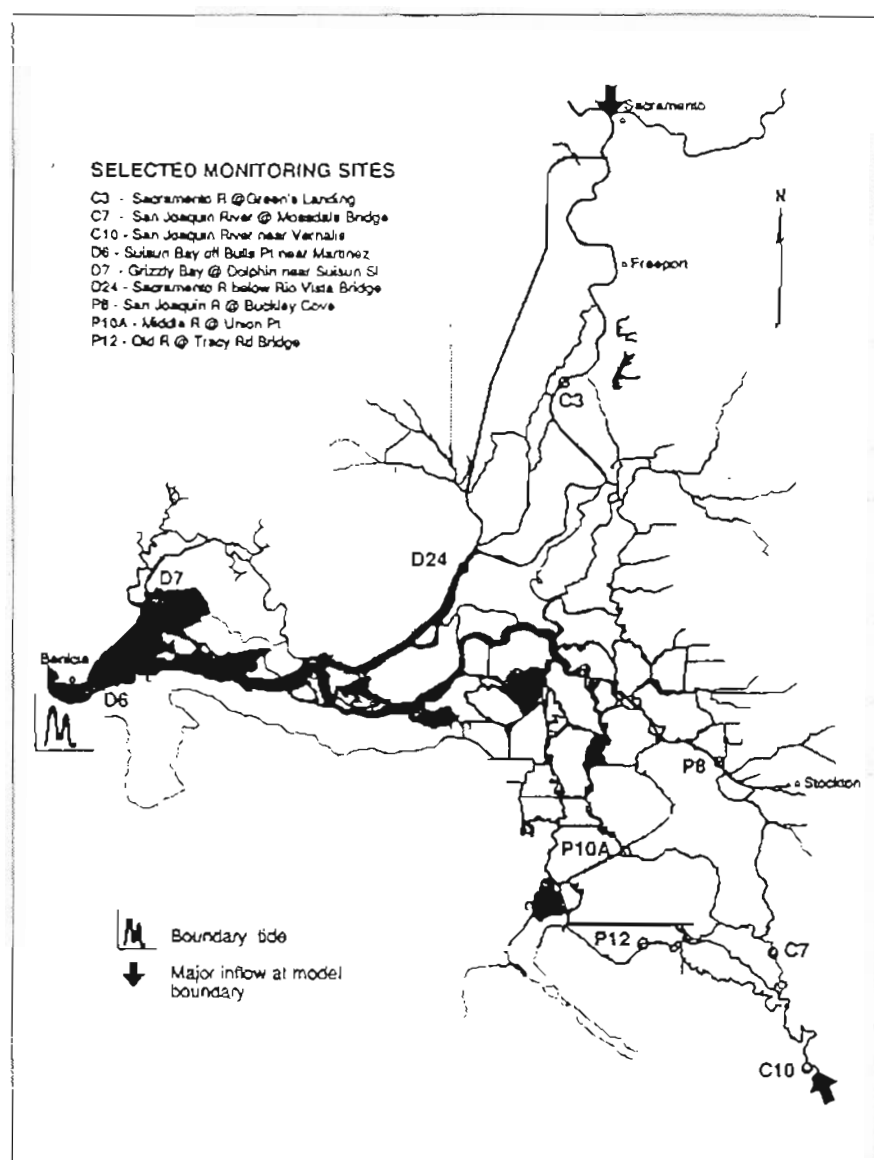


Figure 3-15. Selected Monitoring Stations in the Sacramento-San Joaquin Delta

Scenario 1: Calibration of The Model

Hydrodynamics. This scenario represents conditions corresponding to September 20, 1988, when there was no barrier at the head of Old River. The actual tide at the Martinez boundary was adjusted so as to repeat each 25 hours. With this tide imposed at the seaward boundary and using the freshwater inflows presented in Table 3-3, the DWRDSM hydrodynamics model was run until a state of hydrodynamic equilibrium was achieved.

Upon examination, the computed stages compared reasonably well at locations near Stockton. The flow split (daily mean) at the head of Old River was close to that actually observed during the time period simulated. Model results showed 83 percent flow into Old River with only 17 percent (260 cfs) passing downstream in the San Joaquin River (Figure 3-19). Figures 3-20 and 3-21 are included to show the variation of channel widths and depths in the river.

Table 3-3. Hydrology Used in Model Calibration and Verification

Inflow/Export	Discharge (cfs)	Discharge (cfs)
	Sep 20, 1988	Oct 12, 1988
Sacramento River	11700	11100
San Joaquin River	1610	1050
Mokelumne River	29	30
State Water Project export	2383	4388
CVP export	4610	4407
Contra Costa Canal export	221	214
Stockton City Effluent	31.6	23.6
Consumptive Use	2048	1260
Net Delta Outflow (computed)	4108	1934

Water Quality. Site-specific calibration of the water quality model was focused on the region of San Joaquin River near the Stockton Ship Channel where relatively more water quality data were available. Using this region for model calibration also provided some unique opportunities to examine the local effects of Stockton's wastewater effluent and the unique hydrodynamic conditions due to the placement of the Old River barrier. Initially, all rate coefficients were set to intermediate values in the ranges suggested in the QUAL2E manual (Brown and Barnwell, 1987), or they were set based on previous modeling experiences in the Delta and other similar estuarine systems (Rajbhandari and Orlob, 1990; Smith D.J., 1988; Hydroqual, 1985). Detailed discussions on the sources of data, ranges and their reliabilities are given in Bowie et al (1985).

Calibration started with comparison of diurnal variations of computed temperature with observed (hourly averaged) data at Rough and Ready Island near Stockton (Channel 20). Adjustments of dust attenuation and evaporation coefficients were made until a reasonable agreement between the temperature patterns was obtained. These coefficients affect water temperatures by increasing or decreasing net shortwave solar radiation input and heat energy losses due to evaporation, respectively. The selected values were within the range suggested in the literature (Brown and Barnwell, 1987; TVA, 1972).

Dissolved oxygen is the most important parameter of interest in the current study, consequently it was the primary constituent to be calibrated. DO was generally observed to be at depressed levels, well below saturation, in the Stockton Ship Channel near the waste water outfall (DWR, 1990).

Calibration for DO involves a trade off between the rates of reaeration and benthic oxygen demand (SOD). Other processes such as photosynthetic oxygen production and chemical-biochemical oxidation also affect oxygen balance but have comparatively minor influences on DO balance in this case. Either or both of these dominant processes (reaeration and benthic demand) may be adjusted to achieve acceptable calibration. The O'Connor-Dobbins reaeration equation was coded in the model (Thomann and Mueller, 1987). It computes reaeration rates based on instantaneous channel velocity and the depth of water derived from hydrodynamic simulation. A minimum rate (as a function of depth) of 3

Table 3-4. Water Quality (Field Data¹) at the Model Boundary
September 1988 Simulation

	Sacramento River at Green's L. (C3) or Freeport	San Joaquin River at Vernalis (C10) or Mossdale ² (C7)	Suisun Bay near Martinez (D6)	Mokelumne River at Woodbridge	Agricultural Return	Stockton City Effluent
Date/Time	Sep 15/0815 Sep 13/1130f	Sep16/0950	Sep21/1255	Sep 14/1120		
TDS	139 f	hourly (450-480)	hourly (16k-21k)	63	1030	900
DO	8.0 f	hourly (7-8)	7.9	8.7 (97% Sat)	5.1	5.3
Organic N	0.5 f	0.3	0.3	0.2	1.4	2.5
NH3-N	0.2	0.01	0.02	0.03	0.31	14.0
NO2+NO3	0.09	1.30	0.37	0.09		
NO2	0.01 e	0.13 e	0.04 e	0.01	0.02	1.46
NO3	0.08 e	1.17 e	0.33 e	0.08	1.3	1.19
Organic P (estimate)	0.03 b	0.11*	0.07 b	0.04	0.09	
Ortho-PO4	0.1 b	0.12*	0.15 b	0.02	0.40	0.66 a
Chlorophyll-a µg/l	0.3	19.1	0.2	0.3	10.0	14.0 a
Temperature °C	20	hourly (18-19)	hourly (18.5-19.5)	21.5	19.6	20.0
BOD					3.9	11.0

- a = 09/20/89
 b = 09/01/88
 e = estimate
 f = Freeport 09/13/88
 * = 09/02/88

¹ Note: All units are in mg/l except when noted. Organic phosphorus was obtained by subtracting ortho-PO4 from total phosphorus. Dissolved nitrite and nitrate were obtained by subdividing their known total into 10 and 90 percent values. Hourly data are also shown by plots (Figures 3-16, 3-17).

² Mossdale data were used as hourly data for the model boundary at Vernalis.

Table 3-5. Water Quality (Field Data¹) at the Model Boundary
October 1988 Simulation

	Sacramento River at Green's Landing (C3) or Freeport	San Joaquin River at Vernalis (C10) or Mosssdale ² (C7)	Suisun Bay near Martinez (D6)	Agricultural Return	Stockton City Effluent
Date/Time	Oct 17/0955 Oct 18/1100f	Oct 18/1210	Oct 5/1300		
TDS	96 f	hourly (498-536)	hourly (14500-23800)	807	1004
DO	8.9 f (96% Sat)	hourly (7.2-8)	hourly (7.8-8.3)	5.3	6.2
Organic N	0.2	0.3	0.3	1.4	3.8
NH3-N	0.51	0.00	0.01	0.31	21.4
NO2+NO3	0.09	1.10	0.34		
NO2	0.01 e	0.10 e	0.03 e	0.02	0.26
NO3	0.08 c	1.0 c	0.31 e	1.3	0.7
Organic P	0.03	0.11	0.18	0.09	
Ortho-PO4	0.18	0.1	0.06	0.40	2.94 ^a
Chlorophyll-a µg/l	0.9	27.6	0.1	10.0	28 ^a
Temperature ° C	19	hourly (18.8-19.6)	hourly (17.7-18.7)	17.3	19.0
BOD				6.0	8.0

a = 10/25/89
e = estimate
f = Freeport

¹ Note: All units are in mg/l except when noted. Organic phosphorus was obtained by subtracting ortho-PO4 from total phosphorus. Dissolved nitrite and nitrate were obtained by subdividing their known total into 10 and 90 percent values. Hourly data are also shown by plots (Figures 3-16, 3-17).

² Mosssdale data were used as hourly data for the model boundary at Vernalis.

Table 3-6. Water Quality (Field Data¹) at Selected Delta Locations
September 1988 Simulation

	Old R. at Tracy Road Bridge (P12)	Middle R. at Union Point (P10A)	Sac R. below Rio Vista Bridge (D24)	Grizzly Bay at Dolphin (D7)
Date/Time	Sep 16/1135	Sep 15/1100	Sep 20/1420	Sep 20/1025
Tide	LH	LH	LH	LH
TDS	527*	257 b	178 (+)	13500 (+)
DO	8.6	7.7	8.3	8.1
Organic N	0.3	0.1	0.4	0.3
NH3-N	0.03	0.04	0.1	0.01
NO2 (estimate)	0.12	0.02	0.03	0.04
NO2+NO3	1.20	0.21	0.27	0.40
NO3 (estimate)	1.08	0.19	0.24	0.36
Organic P (estimate)	0.10*	0.03 b	0.03(+)	0.10
Ortho-PO4	0.14*	0.08 b	0.11(+)	0.18 (+)
Chlorophyll-a mg/l	26	2.4	2.1	1.2
Temperature °C	20	21	20	18 °C
BOD				

b = 09/1/88 data
 * = 09/2/88 data
 (+) = 09/6/88 data

¹ Note: All units are in mg/l except when noted. Organic phosphorus was obtained by subtracting Ortho-PO4 from total phosphorus. Dissolved nitrite and nitrate were obtained by subdividing their known total into 10 and 90 percent values.

**Table 3-7. Water Quality (Field Data¹) at Selected Delta Locations
October 1988 Simulation**

	Old R. at Tracy Road Bridge (P12)	Middle R. at Union Point (P10A)	Sac R. below Rio Vista Bridge (D24)	Grizzly Bay at Dolphin (D7)
Date/Time	Oct 18/1435	Oct 17/1240	Oct 19/1325	Oct 19/1015
Tide	LH	LH	LH	LH
TDS	591 (+)	270 b	335 (+)	13200 (+)
DO	8.7	7.8	8.1	7.8
Organic N	0.4	0.2	0.1	0.2
NH3-N	0.00	0.07	0.07	0.00
NO2 (estimate)	0.09	0.03	0.02	0.04
NO2+NO3	0.93	0.32	0.22	0.43
NO3 (estimate)	0.84	0.29	0.20	0.39
Organic P (estimate)	0.09	0.03	0.06 (+)	0.14 (+)
Ortho-PO4	0.12	0.10	0.07 (+)	0.12 (+)
Chlorophyll-a, µg/l	39.2	1.4	2.5	0.8
Temperature °C	21	21	20	19
BOD				

b = 10/03/88

* = 10/03/88

(+) = 10/04/88

¹ Note: All units are in mg/l except when noted. Organic phosphorus was obtained by subtracting ortho-PO4 from total phosphorus. Dissolved nitrite and nitrate were obtained by subdividing their known total into 10 and 90 percent values.

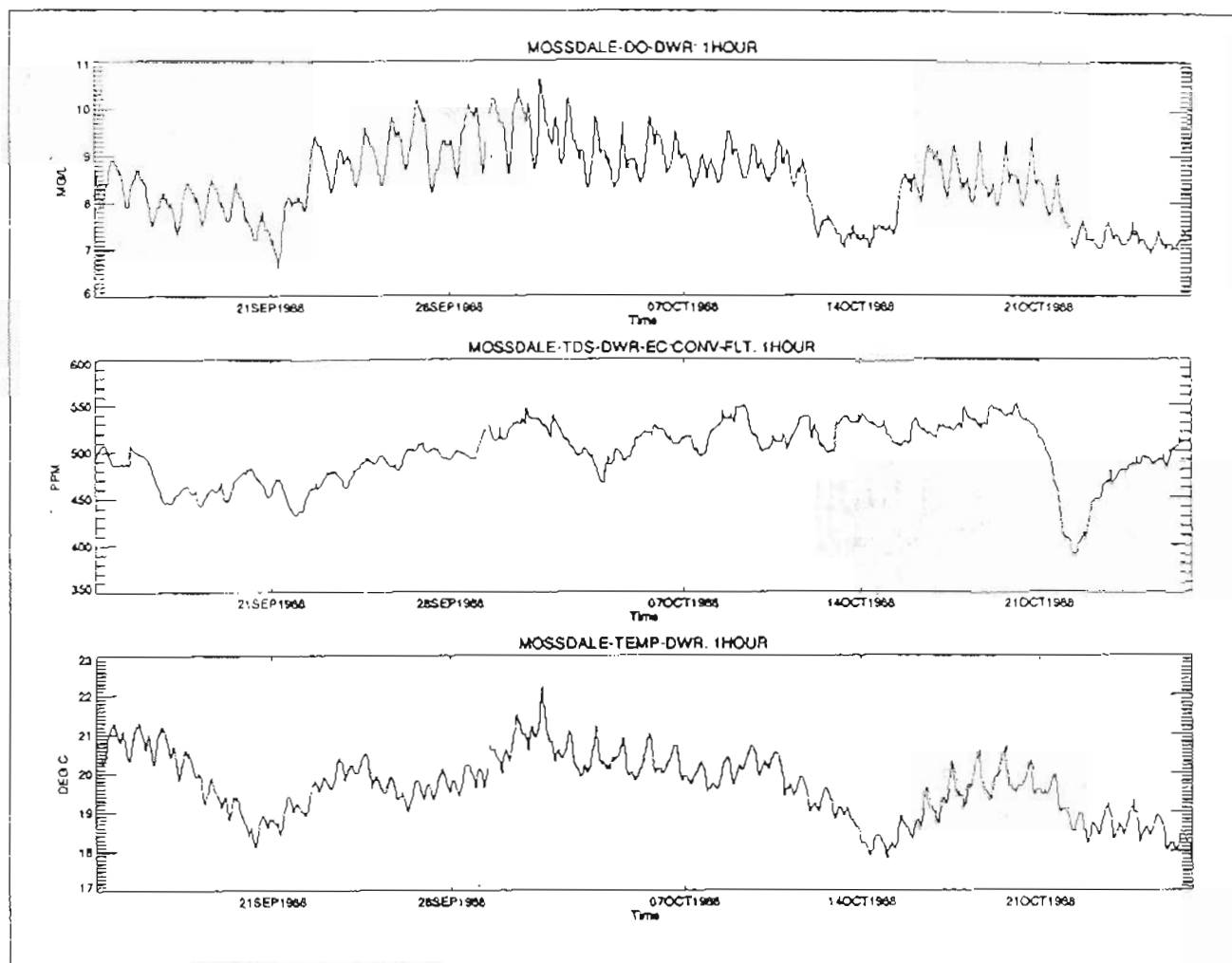
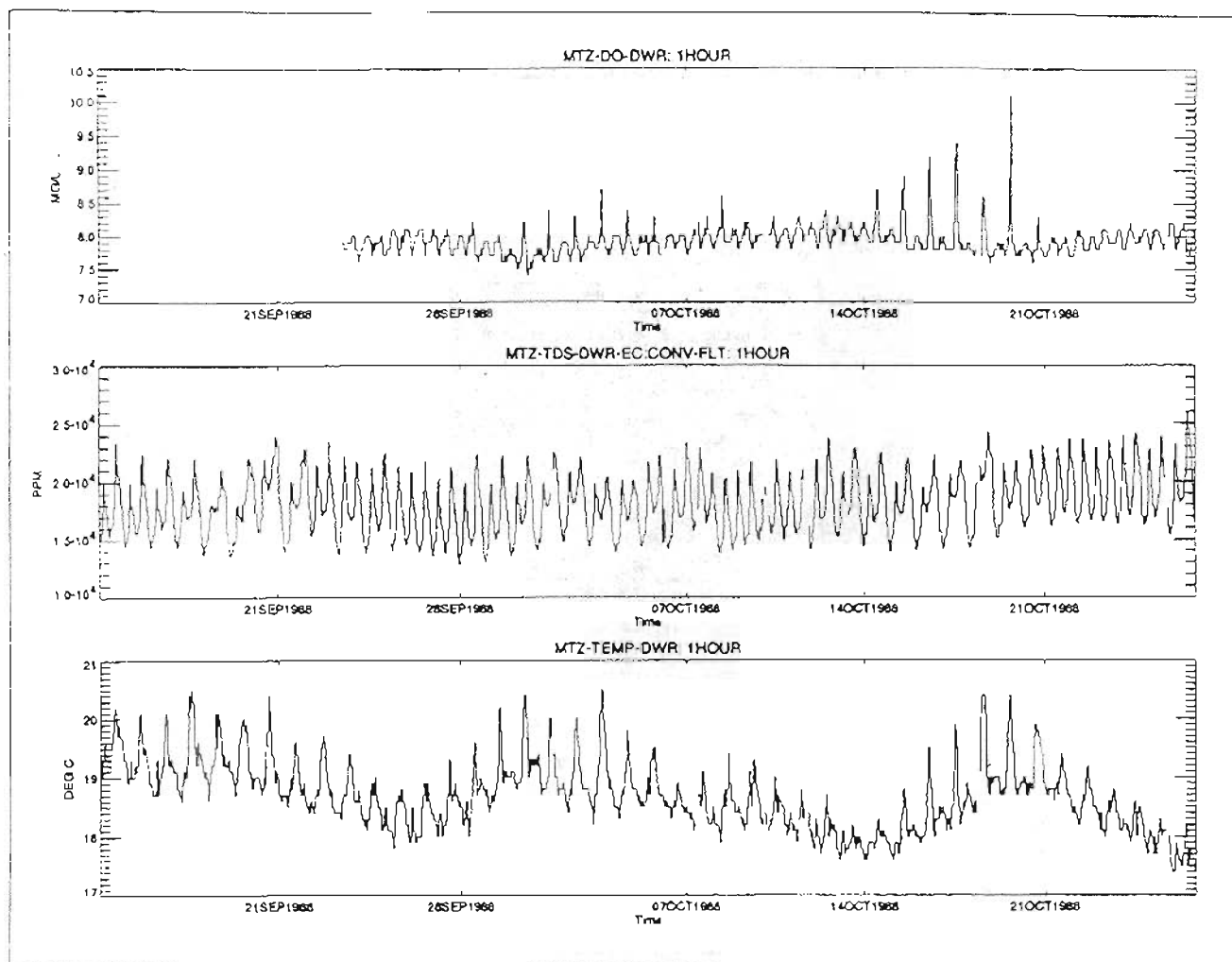


Figure 3-16. Dissolved Oxygen, Total Dissolved Solids, and Temperature at Martinez (September 14 to October 24, 1988)

ft/depth (in feet) per day was adapted to account for reaeration during very low velocities during slack tide conditions.

In calibration there was generally more latitude for adjustment in DO by varying benthic demands, although these were only varied spatially, not temporally. In areas near the effluent outfall site, SOD is expected to be higher because deposits of settleable organic solids tend to build up over time, especially due to historically poor circulation of water in the area, most notable during extended droughts. During the calibration process various values of the benthic oxygen demand based on the suggested range of 2–10.0 g/m²–day (Thomann, 1972) were tried.

After repeated simulations, adjustments of parameters, and examination of DO profiles from the downstream end of channel 10 (approximately 20 miles downstream of Vernalis) to channel 31 (approximately 38 miles downstream of Vernalis), model results were found to be in good agreement with field data. The calibrated model uses benthic oxygen demands of 1.6 g/m²–day for channels 1 through 9 and 4.9 g/m²–day from channels 10 through 20 (in the vicinity of the outfall). A uniform demand rate of 0.5 g/m²–day was assigned to the rest of the Delta.



**Figure 3-17. Dissolved Oxygen, Total Dissolved Solids, and Temperature
in the San Joaquin River at Mossdale
(September 14 to October 24, 1988)**

Profiles of calibrated DO and temperature are shown in Figures 3-22a and 3-23a. The time variation of computed discharge at channel 13 is shown as an inset in the DO plot.

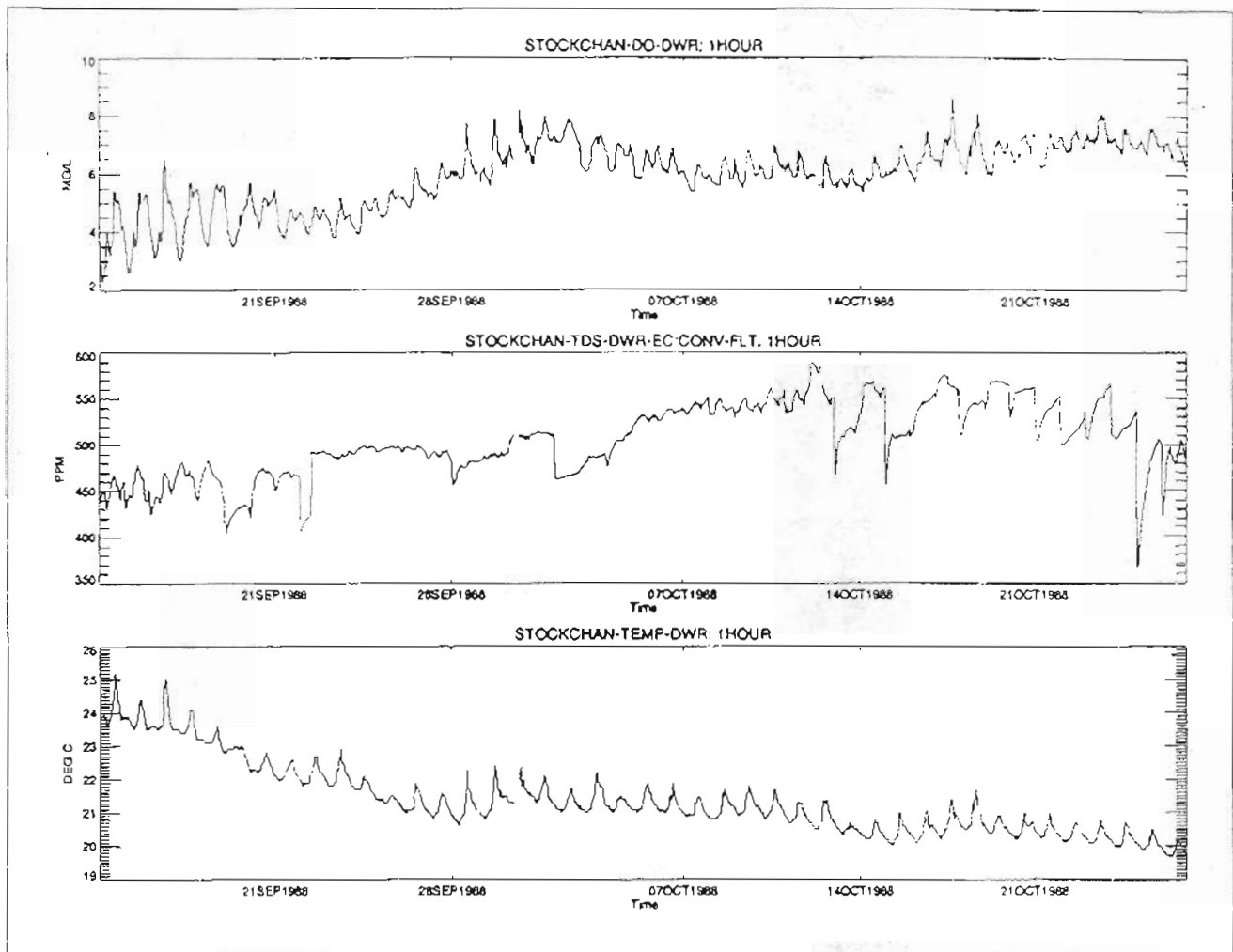


Figure 3-18. Dissolved Oxygen, Total Dissolved Solids, and Temperature
in the San Joaquin River at Stockton
(September 14 to October 24, 1988)

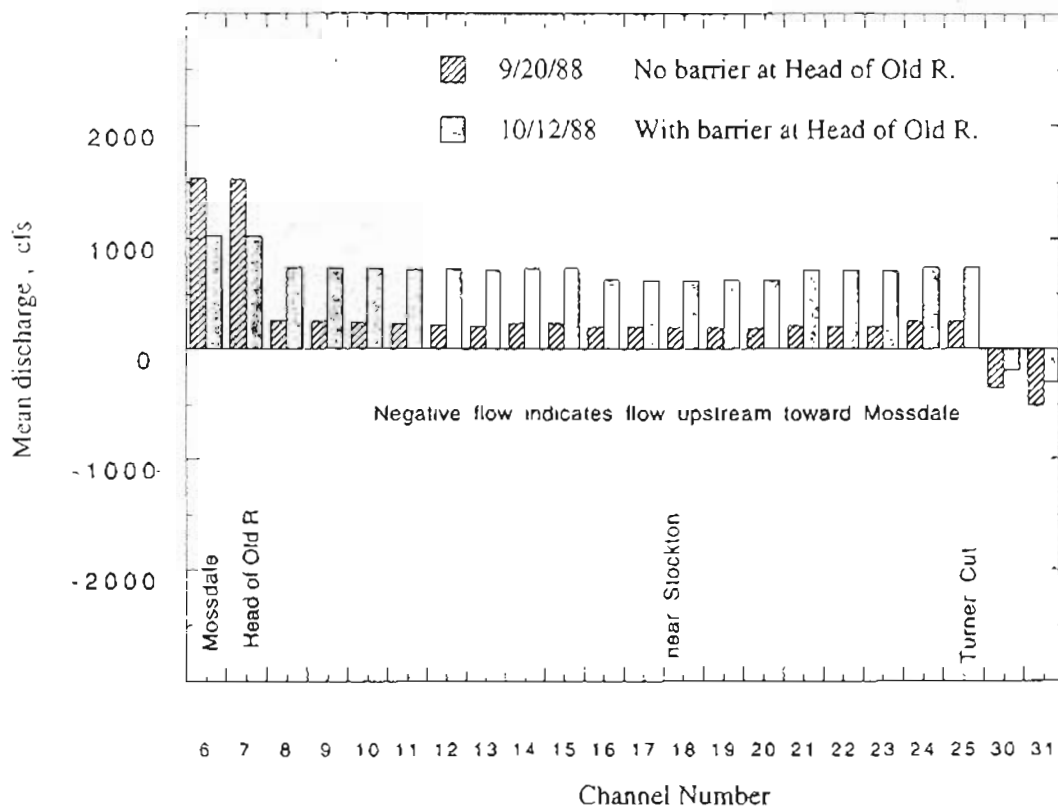


Figure 3-19. Computed Flows (tidally averaged) in the San Joaquin River

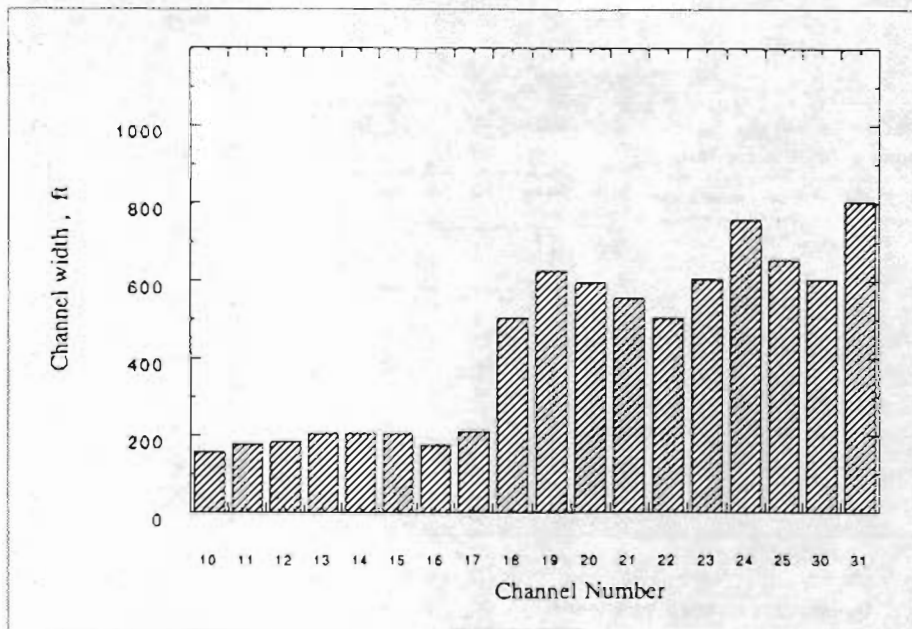


Figure 3-20. Channel Widths along the San Joaquin River

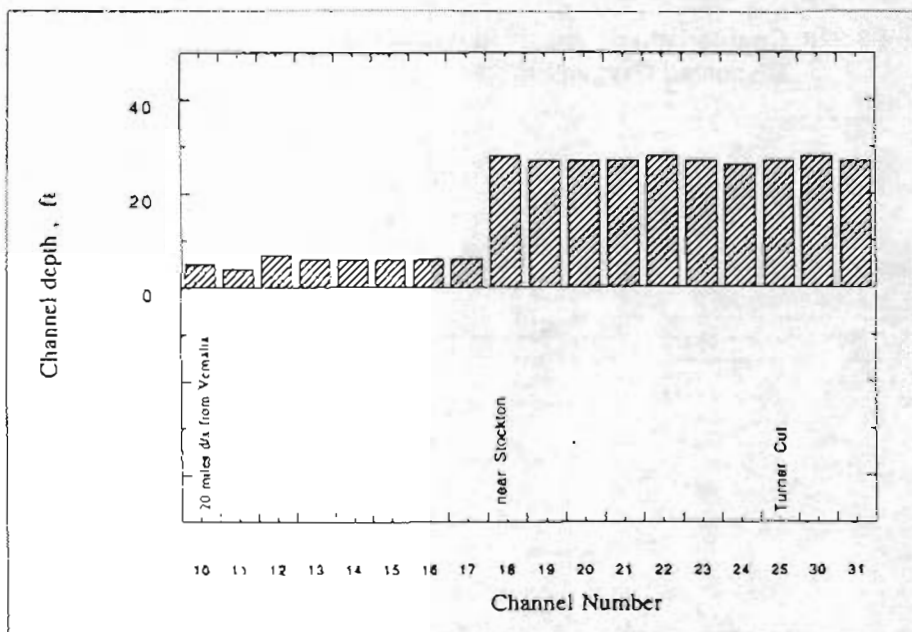


Figure 3-21. Channel Depths along the San Joaquin River

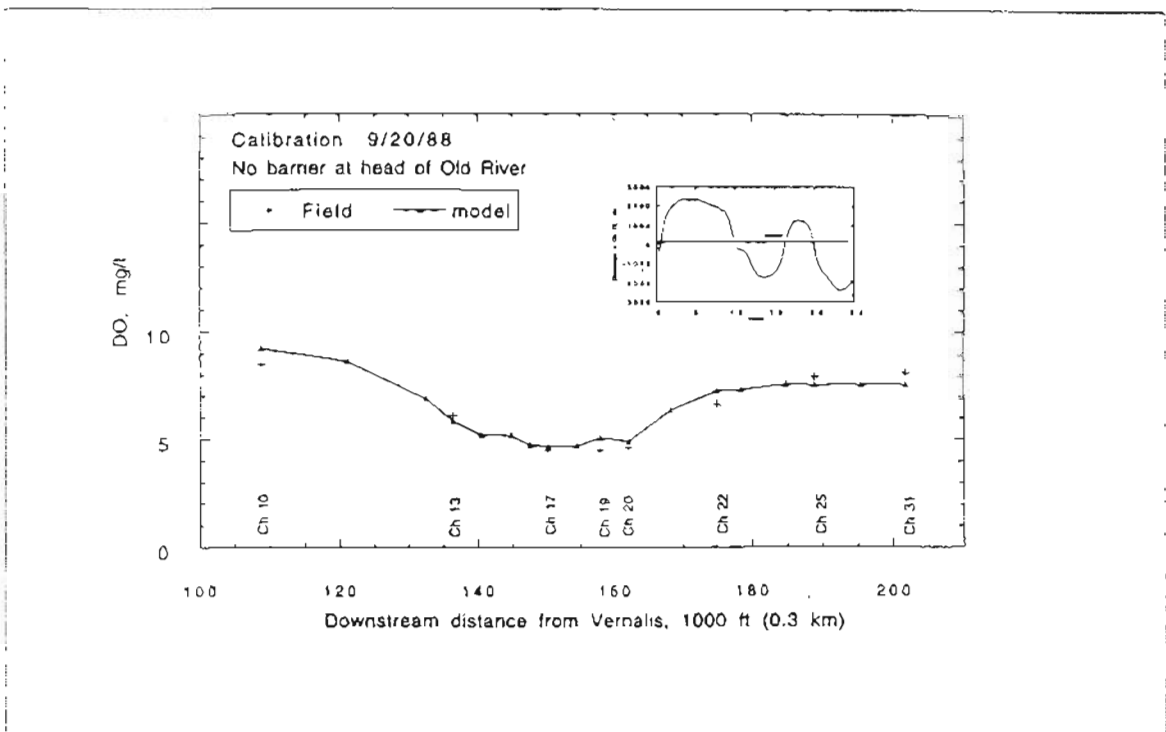


Figure 3-22a. Comparison of Observed and Simulated Dissolved Oxygen Profiles

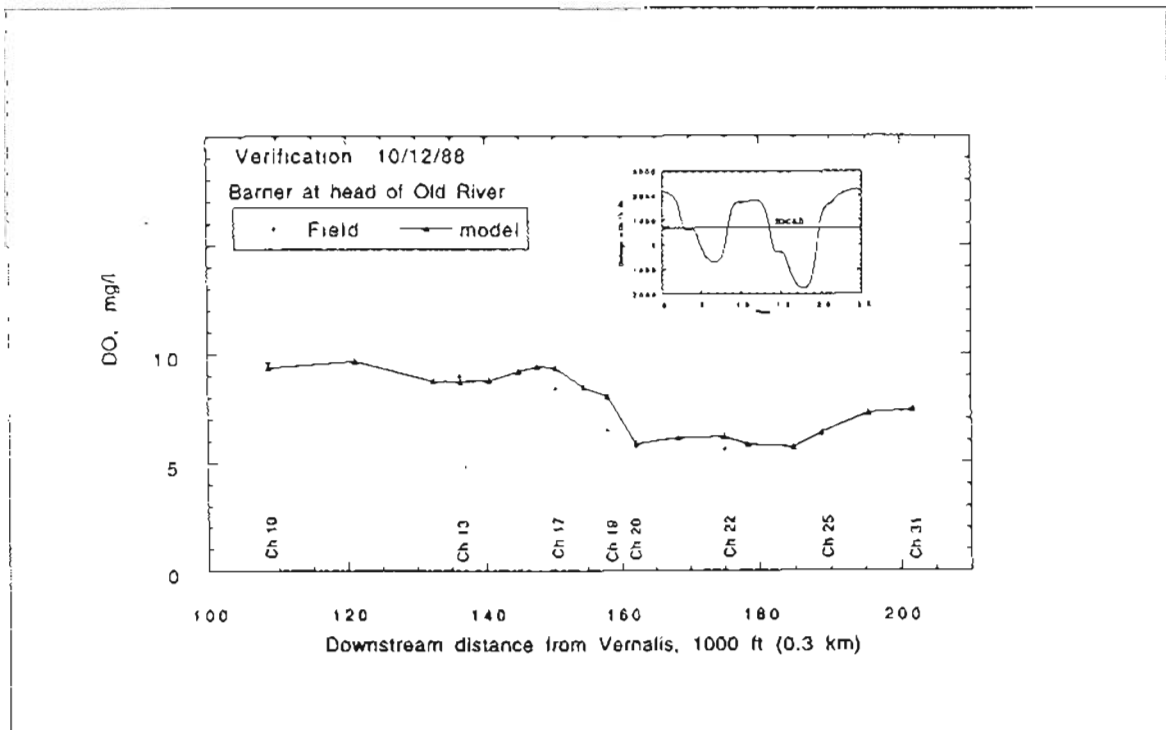


Figure 3-22b. Comparison of Observed and Simulated Dissolved Oxygen Profiles

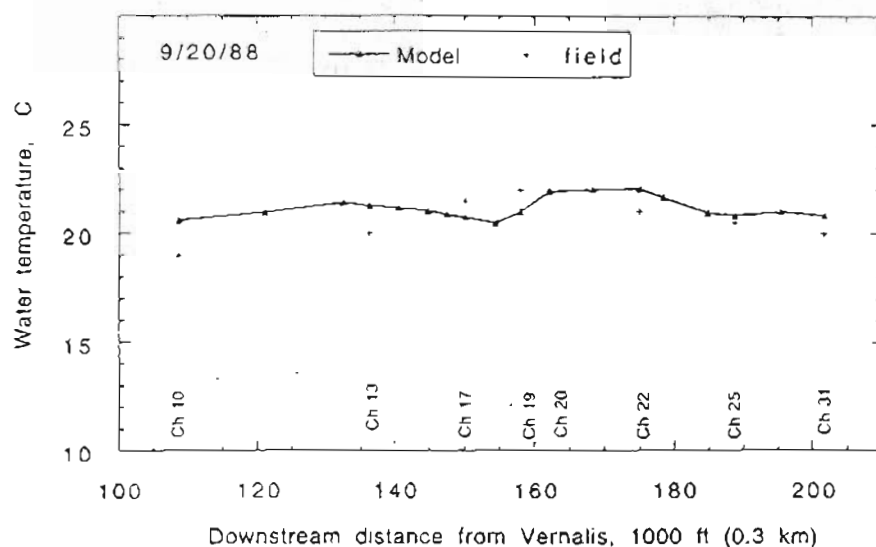


Figure 3-23a. Comparison of Observed and Simulated Temperature Profiles

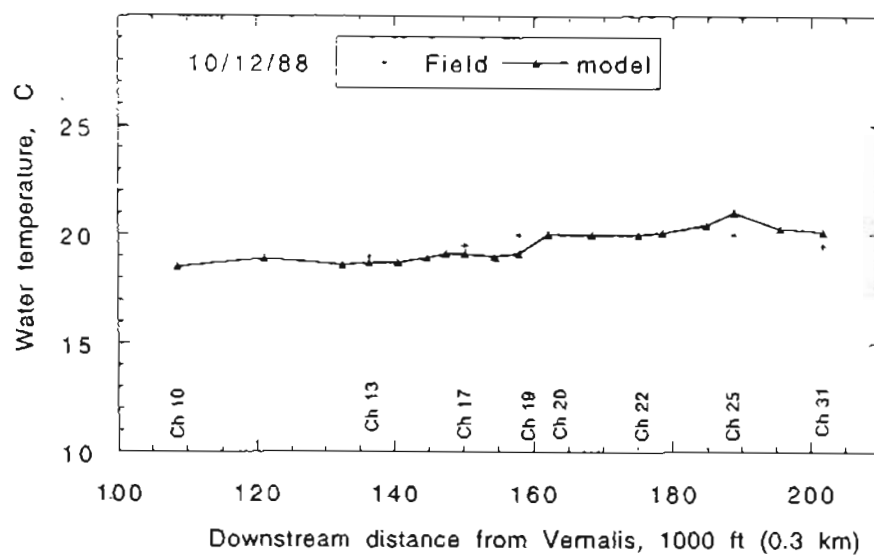


Figure 3-23b. Comparison of Observed and Simulated Temperature Profiles

Scenario 2: Verification of The Model

Hydrodynamics. Following calibration the model was set up to simulate water quality for October 12, 1988. Prior to this date, a rock barrier was put in place at the head of Old River. As in the calibration run the actual tide at the Martinez boundary for this date was adjusted so as to repeat after 25 hours. With this tide imposed at the seaward boundary and using the freshwater inflows presented in Table 3-3, the DWRDSM hydrodynamics module was run until a state of dynamic equilibrium was achieved.

The flow split at the Old River Head computed by the model was found to be close to that actually observed during the same time period. Model results showed the flow split (daily mean) into Old River at its head to be 27 percent (280 cfs), with 73 percent (741 cfs) of the flow passing downstream in the San Joaquin River. This represents a nearly three-fold increase in the net downstream flow over that of September 20, 1988 simulation period (see Figure 3-19).

Water Quality. In this simulation calibration coefficients previously established remain unaltered. This allows us to examine how well the model can simulate hydrodynamic and water quality conditions different from those of the calibration period, a measure of the model's reliability as a simulation tool.

Figure 3-22b represents the comparison of computed DO and field data for the verification run. Model results agree very closely with field observations over the 18-mile reach of the river, reproducing most features of the "oxygen sag". Especially notable is the displacement of the sag downstream due to the increase in net downstream flow (compared to the calibration case) and the increase in the DO sag minimum, due apparently to improved reaeration and dispersion along the channel. A comparison of temperature profiles which look reasonable, especially considering the fact that one set of climate data was used for the entire system, is shown in Figure 3-23b. (This study used data from Sacramento Airport Station for lack of detailed data at Stockton Station, although the latter would have been more appropriate because of the focus in this region for the present evaluation).

Figure 3-24 shows the profiles of nitrate-nitrogen during the two simulation periods. Ranges of observed data for the months of September and October 1988 (taken at weekly intervals) are shown for comparison. Nitrate is somewhat underestimated by the model, due, most likely, to uncertainties in boundary values. Future modeling efforts are expected to improve nitrate simulation capability.

Figures 3-25 and 3-26 present computed profiles of chlorophyll-a and orthophosphate of the reach for the two simulation periods. In these plots, field data at only one station (P8) were available for comparison.

Diurnal Variation in Water Quality. The diurnal variation of DO is important because it informs us how low DO levels can get during certain hours of the daily cycle. This variation can be significant when larger populations of algae are present in the water. Figures 3-27 through 3-33 show diurnal variations of selected quality variables at a station near Stockton (Channel 17) for the September 1988 scenario. The chlorophyll pattern shown in Figure 3-27 is typical of what would be expected on a clear day. The sinusoidal pattern seen for afternoon hours shows the influence of solar radiation that peaks during mid-afternoon. DO concentrations (shown in Figure 3-28) exhibit a similar trend in concentration variations with elevated levels during the afternoon. This pattern reflects the effect of the increase in photosynthetic oxygen production during afternoon hours. Increased chlorophyll-a levels in the system also deplete nutrients in the system rapidly which, in turn, reduce the demand on oxidation. This process also contributes to the rise of DO levels during the afternoon.

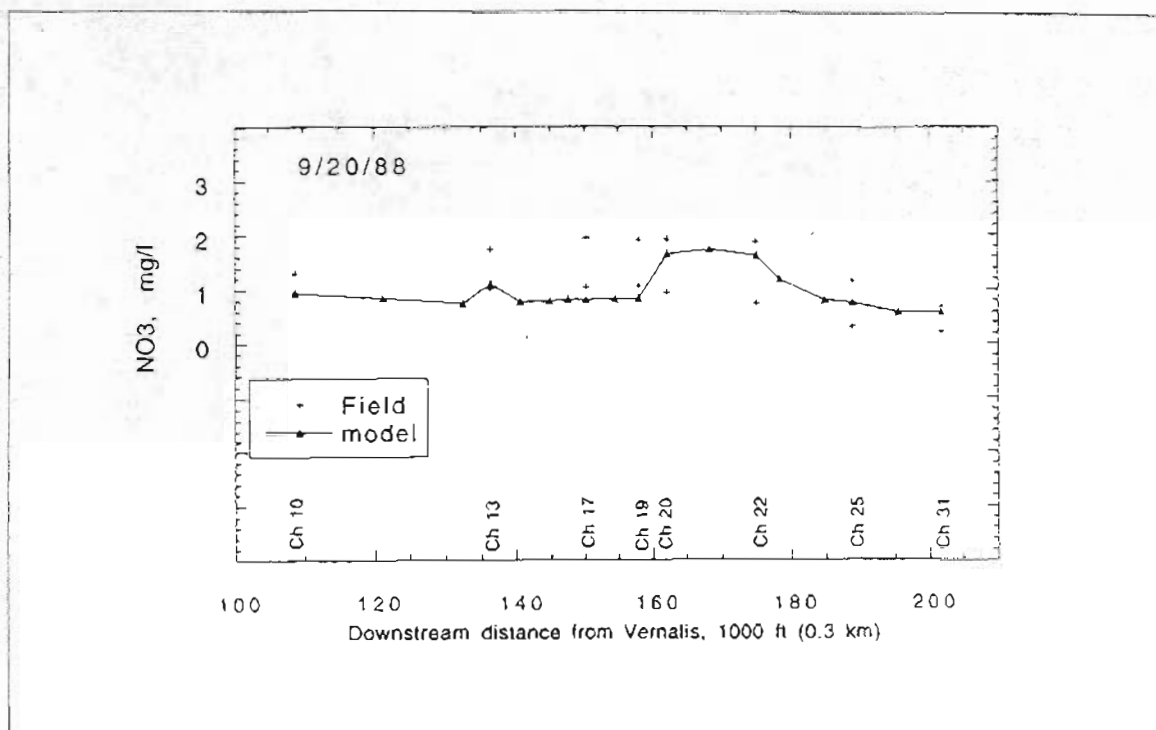


Figure 3-24a. Comparison of Observed and Simulated Nitrate Profiles

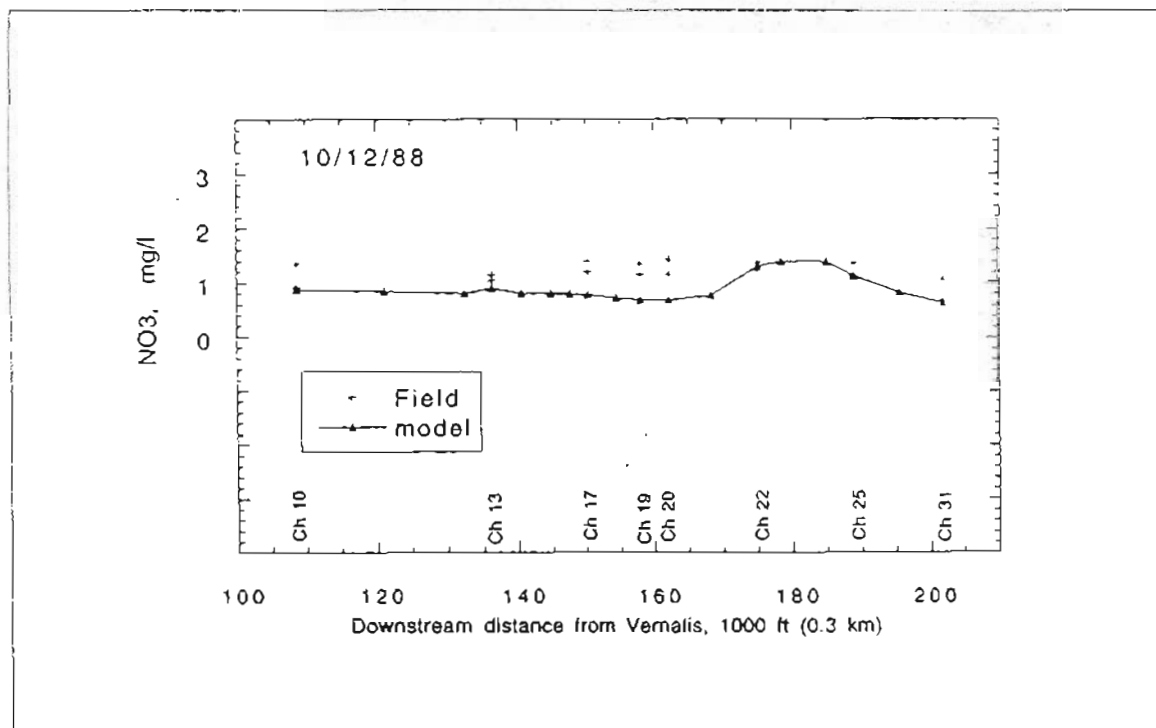


Figure 3-24b. Comparison of Observed and Simulated Nitrate Profiles

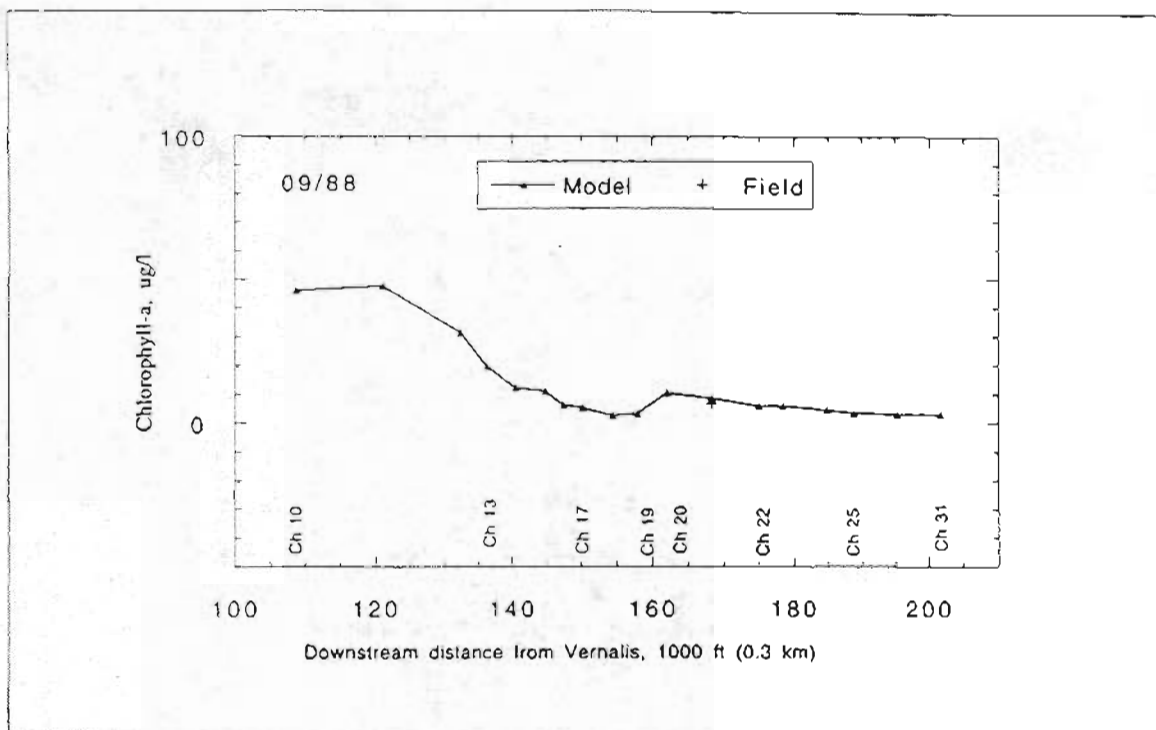


Figure 3-25a. Simulated Chlorophyll-a Profile

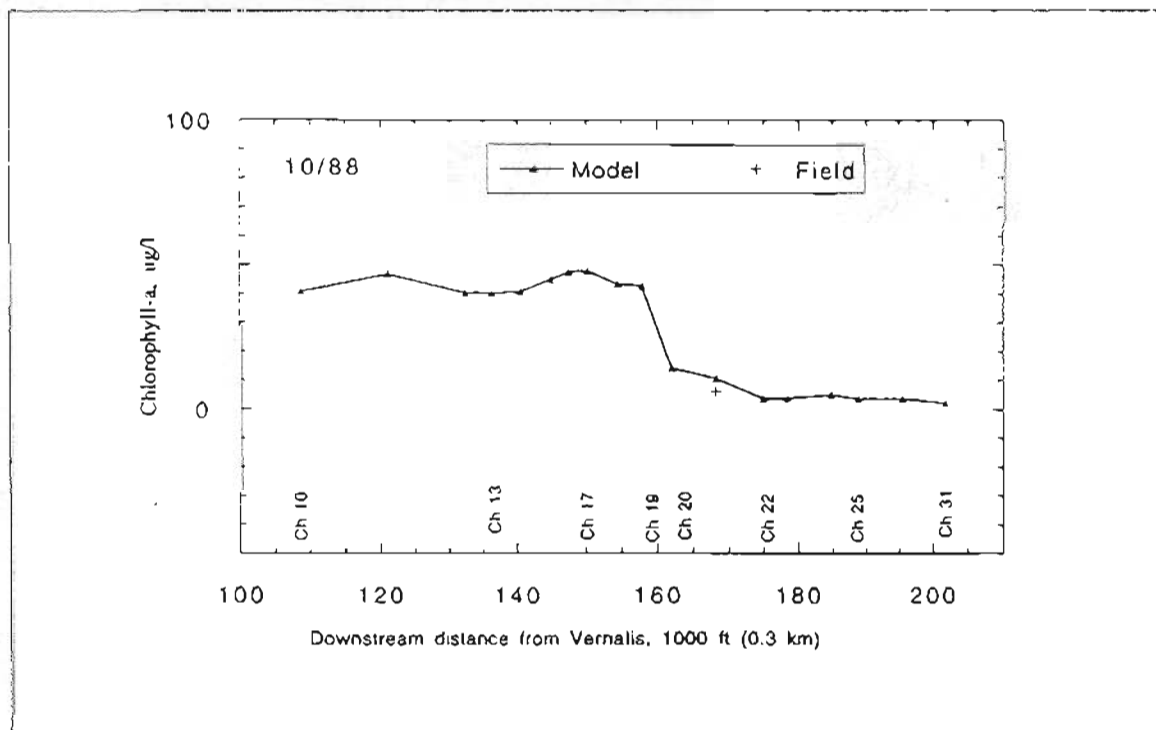


Figure 3-25b. Simulated Chlorophyll-a Profile

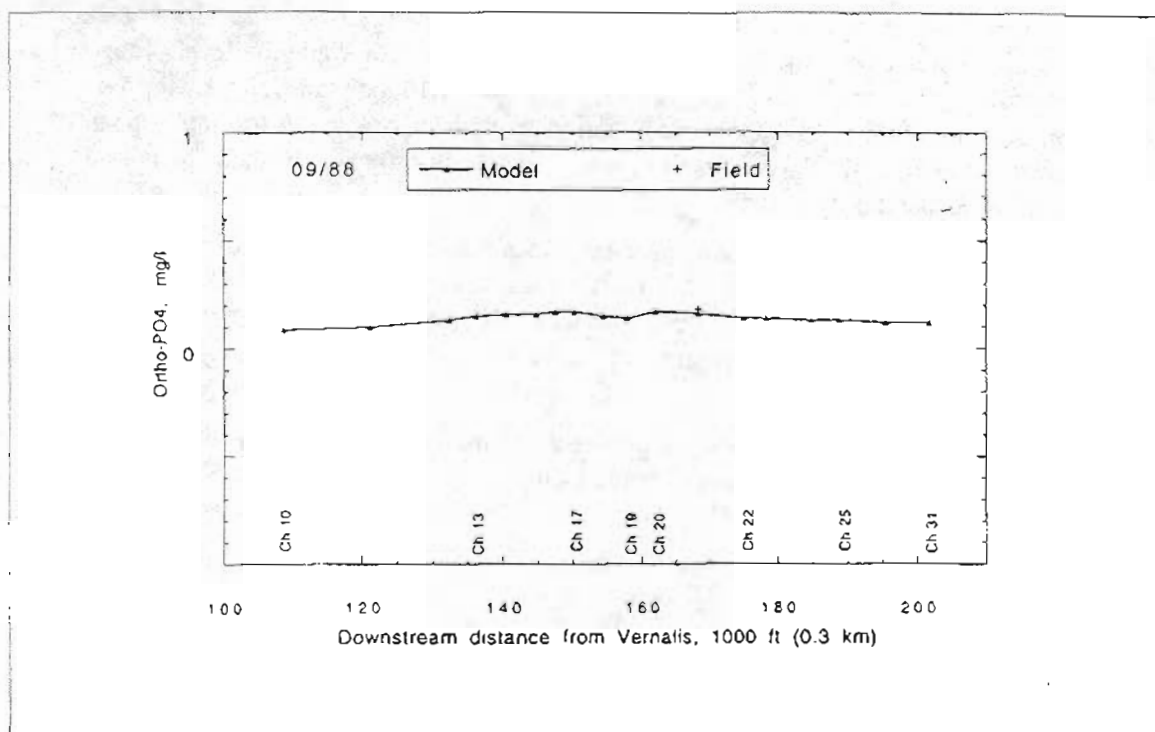


Figure 3-26a. Simulated Orthophosphate Profile

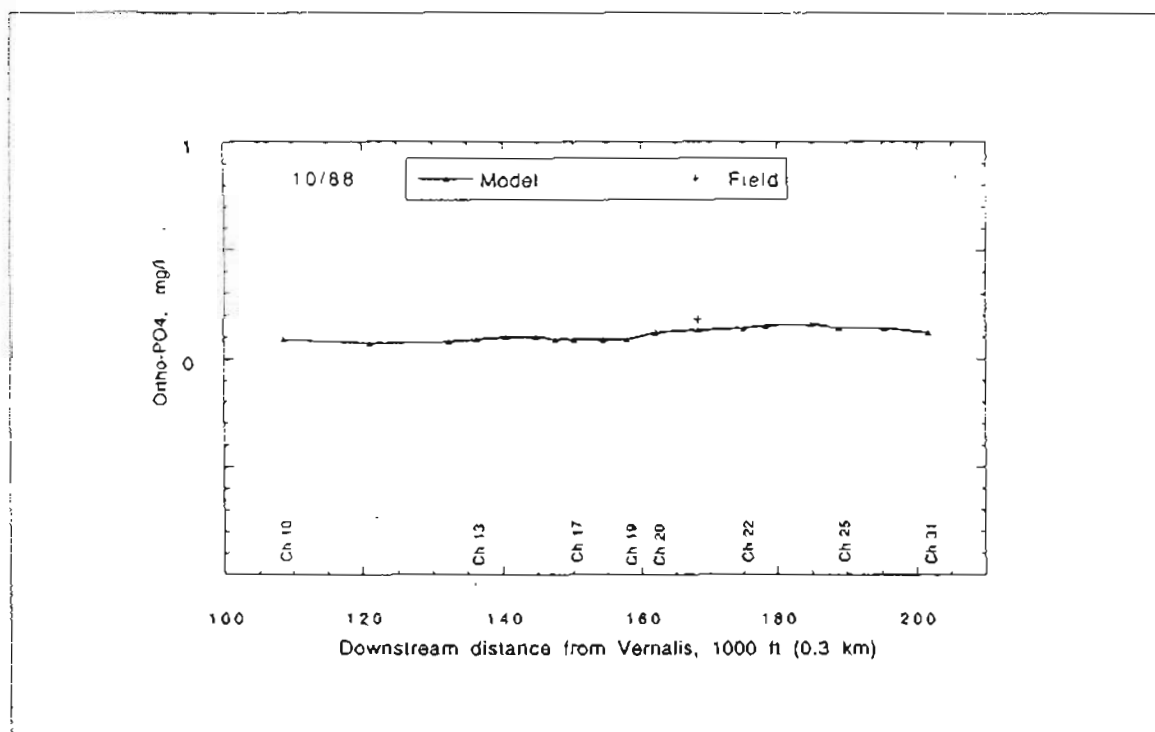


Figure 3-26b. Simulated Orthophosphate Profile

Hourly variations of ammonia and nitrate concentrations (see Figures 3-29 and 3-31) show gradual depression during the hours that correspond to rising chlorophyll-a levels, most likely resulting from the increased uptake rates of nitrogen to maintain cell growth. A similar trend is exhibited by the diurnal pattern of inorganic phosphorus (orthophosphate) as shown in Figure 3-32. The fall in phosphate concentrations results from the increased phosphorus uptake during growth.

Figure 3-30 shows computed organic nitrogen concentrations over a 24-hour period. The rise and fall pattern follows that of chlorophyll-a resulting from the increased release of algal cells during respiration. The hourly variation of computed temperature is included for reference (see Figure 3-33). Note that all of the above transformation processes are dependent on temperature.

Further work on model evaluation is in progress. Future modeling efforts will involve more detailed calibration of the model in the Delta.

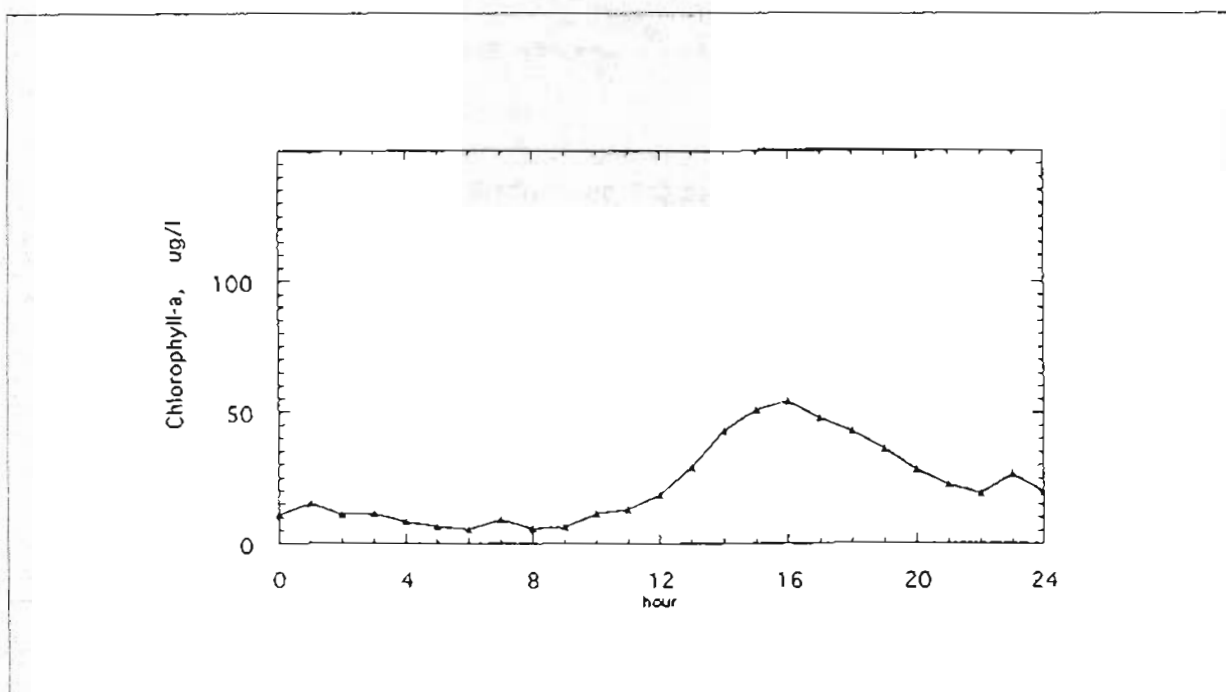


Figure 3-27. Computer Hourly Variation of Chlorophyll-a at Channel 17

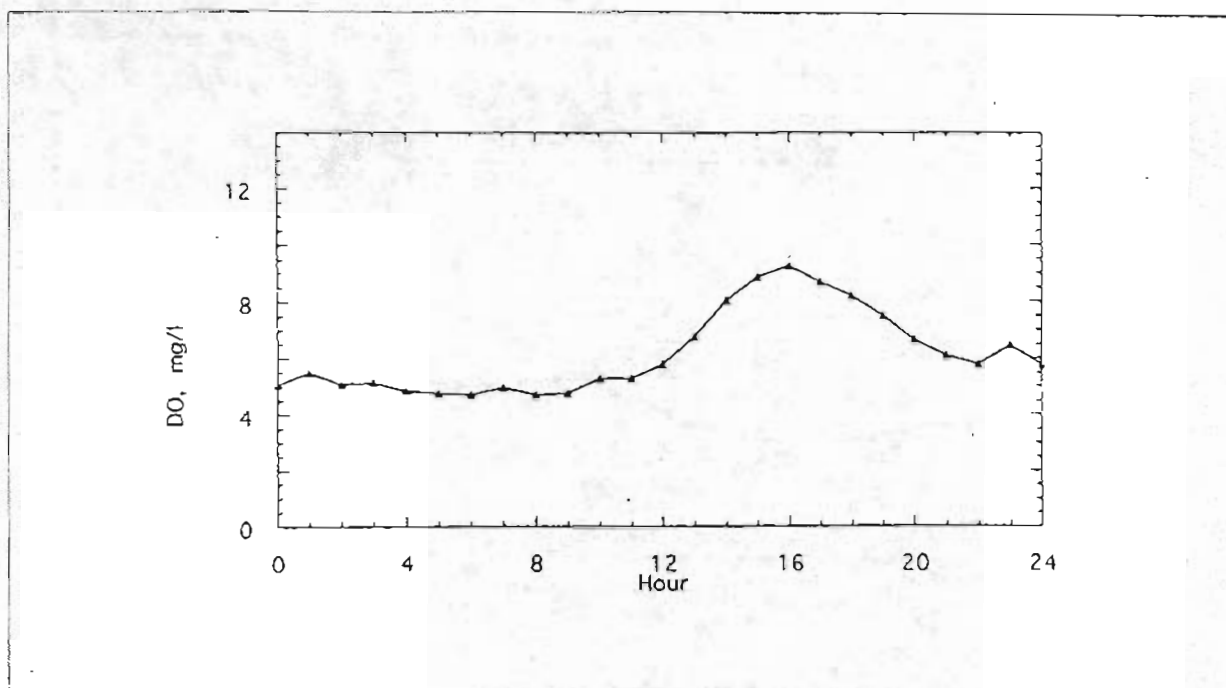


Figure 3-28. Computer Hourly Variation of Dissolved Oxygen at Channel 17

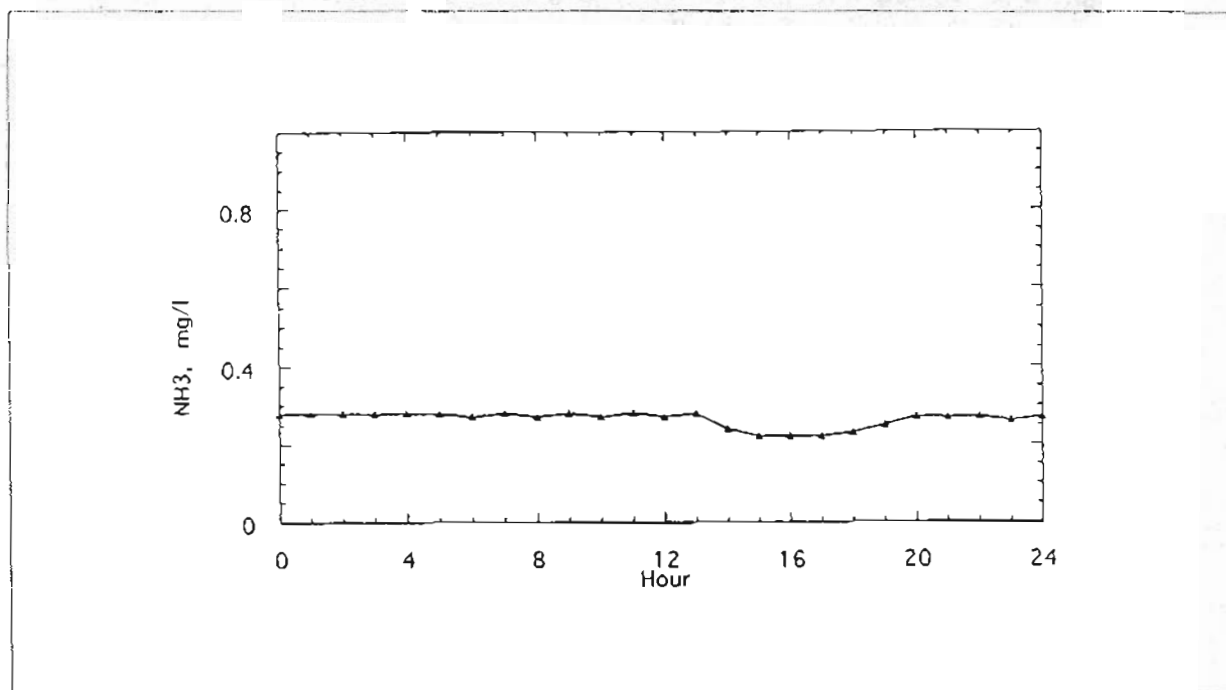


Figure 3-29. Computer Hourly Variation of Ammonia at Channel 17

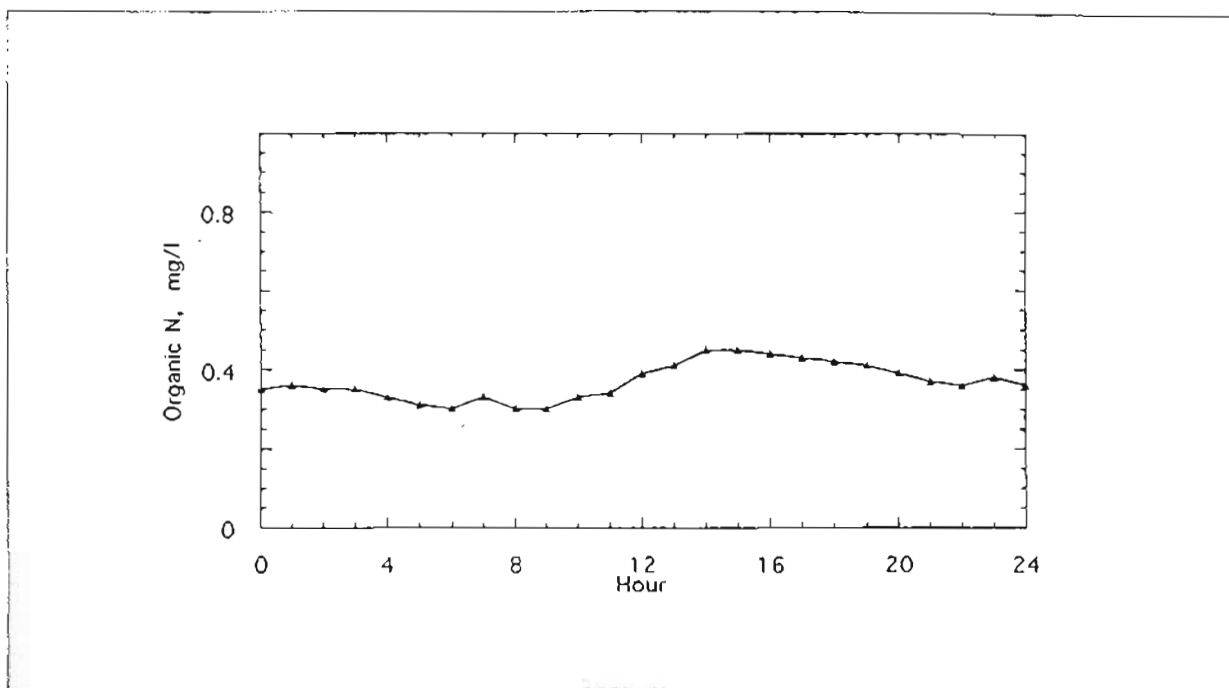


Figure 3-30. Computer Hourly Variation of Organic Nitrogen at Channel 17

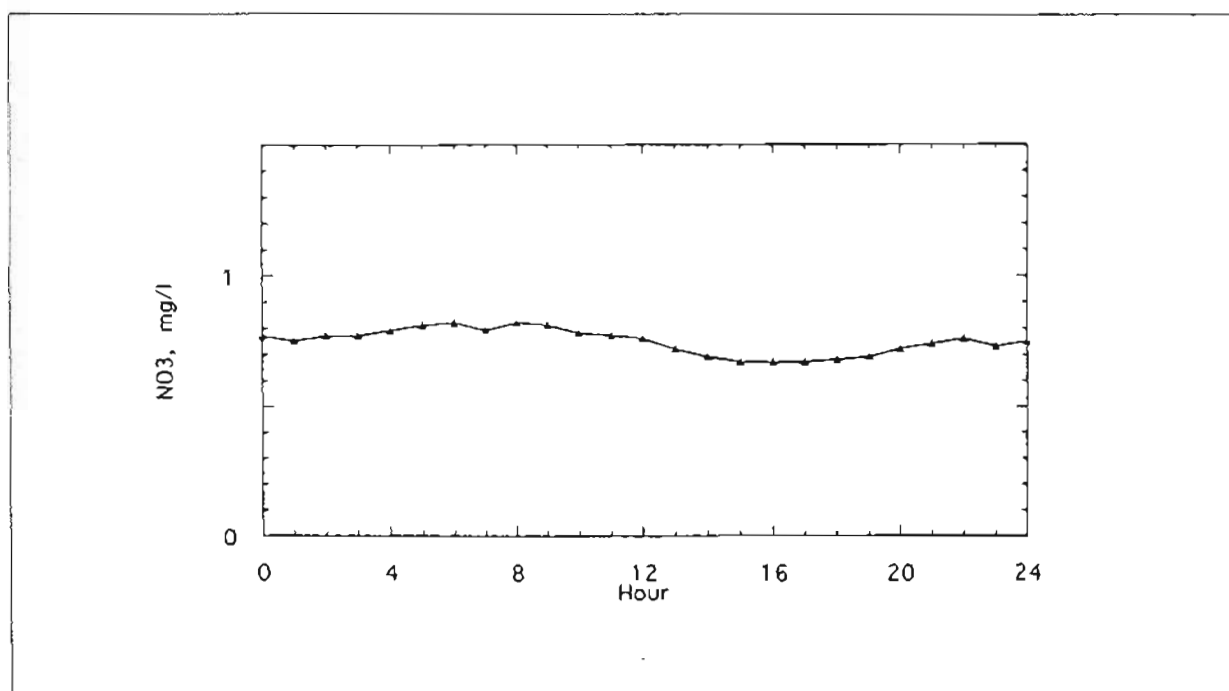


Figure 3-31. Computer Hourly Variation of Nitrate at Channel 17

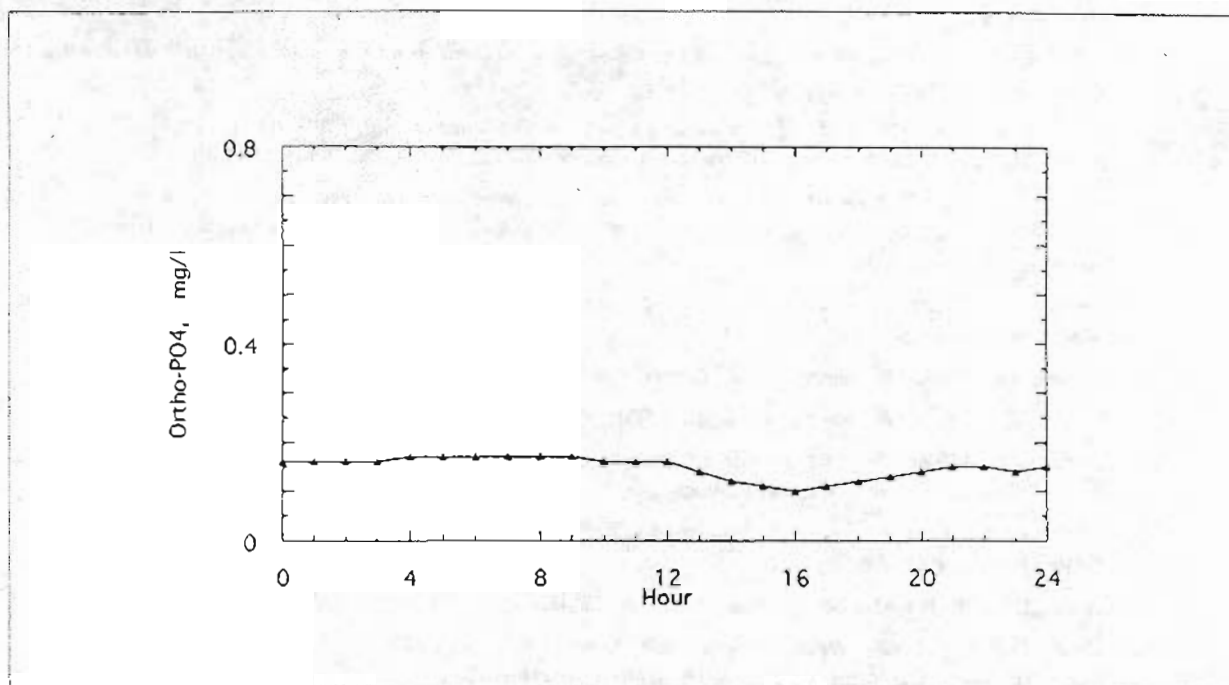


Figure 3-32. Computer Hourly Variation of Orthophosphate at Channel 17

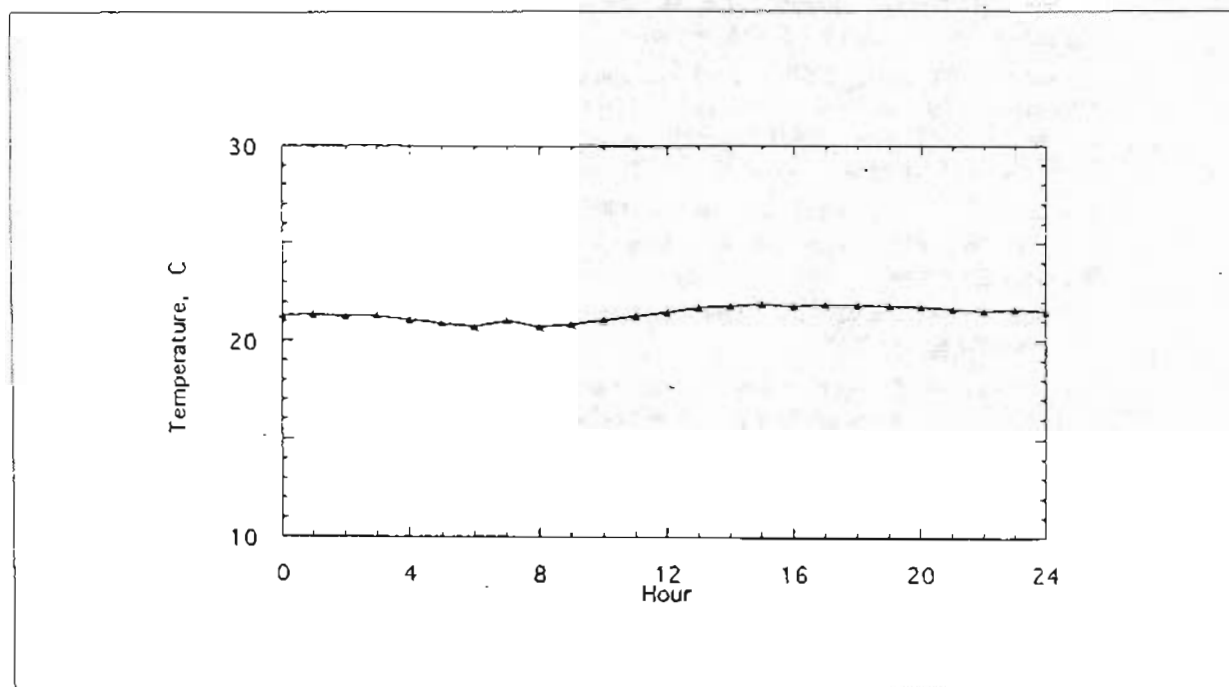


Figure 3-33. Computer Hourly Variation of Temperature at Channel 17

References

- APHA (American Public Health Association)., 1985 *Standard Methods for the Examination of Water and Waste Water*. 16th ed., Washington, D.C. p.874 .
- Bowie, G.L. et al., 1985 *Rates, Constants and Kinetics Formulations in Surface Water Quality Modeling*. Second Edition. U.S. Environmental Protection Agency, Athens, Georgia. EPA 600/3-85/40
- Brown, L.C. and T.O. Barnwell, Jr., 1987. *The Enhanced Stream Water Quality Models QUAL2E and QUAL2E-UNCAS. Documentation and Users Manual*. U.S. Environmental Protection Agency, Athens, Georgia, EPA 600/3-87/007.
- Department of Water Resources. 1990 *Water Quality Conditions in the Sacramento-San Joaquin Delta During 1988*. Division of Local Assistance
- Department of Water Resources. 1967. *Delta and Suisun Marsh Water Quality Investigation. Bulletin 123*
- Department of Water Resources. 1988 *State Water Project Operations Data. Monthly reports*.
- Department of Water Resources. 1990 *Sacramento-San Joaquin Delta Water Quality Surveillance Program -- 1988: Volume 1*. Division of Local Assistance.
- Gromiec, M.J. Reaeration. Ch.3 in. *Mathematical Submodels in Water Quality Systems*. S.E. Jorgensen and M.J. Gromiec (eds.). Elsevier.
- Huber, L. 1995. Personal communication and fax. Department of Municipal Utilities, City of Stockton
- HydroQual. 1985 *Central Delta Eutrophication Model-Multiple Algal Species*. Prepared for the Department of Water Resources, California. HydroQual, Inc., Mahwah, NJ 07430.
- MWQI Data Request. 1995. Internal DWR memorandums to P. Hutton from R. Woodard. February 1 and 15
- National Oceanic and Atmospheric Administration, NOAA. (1988) Local climatological data.
- O'Connor, D.J. and W.E. Dobbins., 1956 *Mechanism of Reaeration in Natural Streams*. J. of the Sanitary Engineering Division, ASCE. 82. SA6. pp 1-30
- Rajbhandari, H. L. and G. T. Orlob., 1990 *Evaluation/ Development of Water Quality Models for Wasteload Allocation in Estuarine Environments*. Prepared for California State Water Resources Control Board and California Regional Water Quality Control Board, San Francisco Bay Region. Department of Civil and Environmental Engineering. University of California, Davis.
- Rajbhandari, H. L., 1995. *Dynamic Simulation of Water Quality Variables in Surface Water Systems Utilizing a Lagrangian Reference Frame*. Ph.D. Dissertation-in-preparation. Department of Civil and Environmental Engineering. University of California, Davis.
- Rathbun, R.E., 1977. *Reaeration Coefficients of Streams. State-of-the-Art*, ASCE, J. Hydraulics Division, Vol. 103, No. HY4, pp. 409-424.
- Smith, D.J. (1988) *Effects of the Stockton Ship Channel Deepening on the Dissolved Oxygen of Water Near the Port of Stockton, California (Phase II)*. Resource Management Associates, Inc., Lafayette, California